Superconducting order parameter symmetry in multilayer cuprates

J. Maly, D. Z. Liu, and K. Levin

Department of Physics, University of Chicago, Chicago, Illinois 60637

(Received 28 August 1995)

We classify the allowed order parameter symmetries in multilayer cuprates and discuss their physical consequences, with emphasis on Josephson tunneling and impurity scattering. Our solutions to the gap equation are based on highly nonspecific forms for the inter- and intraplane pairing interactions in order to arrive at the most general conclusions. Within this framework, the bilayer ($N=2$) case is discussed in detail with reference to Y-Ba-Cu-O (YBCO) and Bi-Sr-Ca-Cu-O (BSCCO) and the related Landau-Ginzburg free energy functional. Particular attention is paid to the role of small orthorhombic distortions as would derive from the chains in YBCO and from superlattice effects in BSCCO, which give rise to a rich and complex behavior of the multilayer order parameter. This order parameter has N components associated with each of the N bands or layers. Moreover, these components have specific phase relationships. In the orthorhombic bilayer case the $(s,-s)$ state is of special interest, since for a wide range of phase space, this state exhibits π phase shifts in corner Josephson junction experiments. In addition, its transition temperature is found to be insensitive to nonmagnetic interplane disorder, as would be present at the rare earth site in YBCO, for example. Of particular interest, also, are the role of van Hove singularities which are seen to stabilize states with $d_{x^2-y^2}$-like symmetry (as well as nodeless s states) and to elongate the gap functions along the four van Hove points, thereby leading to a substantial region of gaplessness. We find that for these rather general models of the pairing interaction the $d_{x^2-y^2}$-like states are the most stable solutions in a large region of parameter space. In this way, they should not be specifically associated with a spin fluctuation driven pairing mechanism.

I. INTRODUCTION

The question of the order parameter symmetry in layered cuprate superconductors is one of the most important issues currently under debate. Despite strong evidence for a $d_{x^2-y^2}$ state,[1] at least in one particular cuprate [Y-Ba-Cu-O (YBCO)], there are still experimental inconsistencies.[2,3] This matter is complicated further by the complexities of YBCO associated with the double copper-oxide plane structure. The same bilayer unit is shared with the bismuth 2212 compounds [Bi-Sr-Ca-Cu-O (BSCCO)], where recent photoemission data,[4,5] seem also to favor a $d_{x^2-y^2}$ symmetry. In the former compound,[6] if not in the latter,[7] there is evidence that the double layer unit leads to two bands each of which crosses the Fermi surface and each of which presumably has a distinct superconducting order parameter. It is not *a priori* clear whether these two gaps have the same or opposite phase, nor whether they are predominantly associated with the same or different irreducible representations of the tetragonal symmetry group. It is, therefore, essential to provide a systematic classification of the order parameter in these bilayer (and more general N-layer) systems before meaningful and unambiguous inferences can be deduced from the experimental data.

It is the purpose of this paper to expand upon earlier work by ourselves[8] and other groups[9–13] by classifying and establishing physical consequences of the various order parameter symmetries in N-layer systems. Of particular interest are those parameter sets which lead to π junction behavior[14–17] in an a,b-plane Josephson configuration. It is widely assumed that the observation of these π phase shifts provides the strongest evidence yet for the $d_{x^2-y^2}$ state in YBCO. By contrast, we find that in the more general orthorhombic bi-

layer case, in part because of van Hove effects,[18] π phase shifts are fairly widespread and not uniquely associated with the $d_{x^2-y^2}$ state. Moreover, the proximity to the van Hove singularities leads to a stabilization of the $d_{x^2-y^2}$ symmetry for a variety of different models for the pairing interaction, beyond the simple spin fluctuation model.[19] It also is associated with a considerable distortion of the gap function away from the ideal representation of the $d_{x^2-y^2}$ state. In order to understand the physical consequences of various order parameter sets we investigate the role of intra- and interlayer impurities, include a discussion of Josephson coupling, and present a more general analysis of our results in the context of both a Landau-Ginzburg theory and the solution of the arbitrary N-layer problem.

A number of authors have considered the possibility of electron tunneling and pair interactions of electrons on different planes in the context of a bilayer structure. Bulut and Scalapino[11] used numerical solutions of a strong coupling model to show that when both interlayer interactions and hopping were included in a bilayer model two competing states arose, one with $d_{x^2-y^2}$ solutions in phase on both subbands of the Fermi surface and the other with s states of opposite sign. Similar observations were made by Liechtenstein and co-workers[9] who argued that the more probable situation for spin fluctuation induced superconductivity, corresponded to a pair of out-of-phase s states. The consequences of such an out-of-phase s state were considered in more detail by Golubov and Mazin.[20] It should be noted that throughout this paper we will use the generic notation "s" (and "d") as applying to gap functions which have the same (or different) signs under a rotation of the wave vector by $\pi/2$. It is important to be particularly clear on our notational convention since we emphasize the role of orthorhombicity

in our work. Among other things, this orthorhombicity leads to what we refer to as "s-d" or "mixed states" (although the overall sign under a $\pi/2$ rotation remains either $+$ or $-$, depending on which component is dominant). The possibility of mixed s-d states has been discussed within Landau-Ginzburg theory, in a monolayer[21] as well as a bilayer context.[22] In the latter, a spontaneous s-d mixing was considered, using microscopic arguments based on a resonating valence bond (RVB) decoupling scheme. While most bilayer studies considered tetragonal symmetry, earlier work by our own group,[8] using the more conventional BCS pairing formulation, investigated the role of a small amount of a,b-axis anisotropy in the bilayer problem. This small orthorhombicity appears to be amplified by van Hove effects. As a consequence, the solution corresponding to a pair of out of phase s-wave states frequently has the interesting and important physical consequence of leading to π phase shifts in a corner Josephson tunneling experiment.[14–17] It should be stressed that orthorhombicity is assumed to enter via the chains in YBCO. There are alternate scenarios for this material which explicitly build in the chain bands[23–25] and their contribution to the superconducting gap. Here we ignore these explicit effects, in large part because recent tunneling studies indicate that the order parameter behavior is largely unaffected by reducing the oxygen stoichiometry to the case of $YBa_2Cu_3O_{6.6}$ in which limit the chains are strongly fragmented.[15] It was argued in Ref. 15 that "this experiment rules out the possibility that the results of previous similar experiments on$YBa_2Cu_3O_{6.9}$ can be explained by the presence of Cu-O chains." Similar observations based on twinning effects have also been made in the theoretical literature. The more general N-layer problem has been studied by Bulaevski and Zyskin[12] as well as Klemm and Liu.[10] In these calculations, it was also assumed that the c axis consisted of a coherently coupled stack of bilayer structural units. Here we presume that the considerable evidence for the absence of c-axis coherence[26,27] requires a different starting point. While, for simplicity, we focus on an isolated N-layer complex, it is clear that higher order effects associated with incoherent coupling between unit cells must ultimately be included. Such incoherent coupling can be introduced following, for example, Ref. 28. An additional complexity was raised in even earlier studies by Efetov and Larkin[29] who pointed out that a complete treatment of interlayer electron pairing required the consideration of a triplet pairing state odd under exchange of layer indices. This case was further investigated by Kettemann and Efetov[13] as well as Klemm and Liu[10] who argued that the mixing of triplet and singlet states would generally lead to a second transition below T_c. Thus far there is no evidence for this second transition, nor is there much support for the triplet pairing state.

There are important issues of controversy implicit in the work discussed here. There appears to be little doubt that the components of the bilayer couple magnetically. However, it has not been persuasively demonstrated that there is a coherent electronic coupling $t_\perp$ within the unit cell.[30] Neutron experiments[31–33] on YBCO provide evidence for a c-axis modulation associated with the spacing of the planes within the bilayer. While this can be explained by magnetic coupling alone,[34,35] photoemission studies on this cuprate have reported the observation of two copper oxide plane bands.[6,36]

The situation in BSCCO is even less certain with two photoemission groups reaching opposite conclusions.[4,7] For the purposes of the present paper it will be assumed that there is coherent coupling between the layers, though not between the unit cells. This assumption is based in large part on the demonstrated intrabilayer magnetic interactions which suggest a moderate degree of communication between the layers. Moreover, on this basis it may be presumed that there are direct or indirect electronic interactions within the bilayer complex which must be included in any complete theory of the superconductivity.

Similarly controversial is the origin of a possible $d_{x^2-y^2}$ state. While this state is consistent with spin fluctuation mediated superconductivity,[1,37] for the models we consider it appears more generally as a solution to the gap equation in the presence of repulsive interactions. Providing this repulsion has some wave-vector dependence [near, although not necessarily pinned at the antiferromagnetic position (π,π)], we find the $d_{x^2-y^2}$ state to be stable. Thus experimental observation of this symmetry appears to provide more support for superconductivity arising from repulsive interactions than for any detailed superconducting mechanism. While there are problems associated with interpreting various experiments within a $d_{x^2-y^2}$ context, among the most perplexing from a theoretical viewpoint[38–40] is the evident impurity insensitivity of the superconducting transition temperature.[41] Moreover, substitution at the rare earth site in YBCO with both magnetic and nonmagnetic atoms, between the planes of the bilayer, leads to no variation in T_c, except in the special case of Pr. Here we address this fascinating puzzle and demonstrate that for the case of two out of phase nodeless s states in an isolated bilayer configuration, Anderson's theorem applies to interplane substitutions. This provides additional motivation for studies of this particular pairing state.

An outline of the paper is as follows. In Sec. II we focus on the bilayer problem as a prototype of the N-layer system. We introduce a generalized model for the pairing interaction (Sec. II A) and then point out some general properties of solutions which arise in these systems (Sec. II B). In Sec. II C we examine the consequences of the bilayer structure on Josephson tunneling experiments between cuprates and conventional superconductors as well as the problem of twinned samples. We then construct (Sec. II D) the free energy functional in the Landau-Ginzburg limit, addressing the effects of interlayer tunneling and orthorhombicity. Impurity scattering will be discussed in Sec. II E, where we investigate the circumstances under which Anderson's theorem holds for the case of two out of phase s states.

In Sec. III we turn to the more technical issues of a general weak coupling treatment of the problem of N two dimensional layers. The reader uninterested in the more mathematical details can skip directly to the conclusions in Sec. IV. The generalized gap equation in the N layer problem is derived (Sec. III A) and the two competing states are discussed in Sec. III B. These correspond to natural analogues of the in-phase and out-of-phase states of the bilayer system. We conclude with a general discussion (Sec. III C) of the role of van Hove effects. Two states are found to take maximal advantage of the van Hove singularities: these are the $d_{x^2-y^2}$ and nodeless s states. Some of the technical aspects

of these calculations as well as a complete solution of the bilayer problem are relegated to Appendixes A and B, respectively.

Our conclusions are presented in Sec. IV.

II. THE $N=2$ CASE

A. Gap equation and model interaction

We initially study the simpler bilayer system ($N=2$) in order to establish notation and to discuss physical results in a more familiar context. Although only singlet intraband pairing is considered in the main part of the text, a more complete weak coupling calculation of the bilayer problem will be presented in Appendix B. Many of the interesting features of bilayers arise in the general N-layer problem with only slight modification. However, this more general case will be discussed in detail in Sec. III. Section II B focuses primarily on the linearized gap equation. Throughout Sec. II, particular attention will be devoted to elucidating the role of orthorhombicity.

The weak coupling gap equations for two copper oxides planes are given by

$$\Delta_+ + \Delta_- = -\sum_{\mathbf{q}} V_\parallel \left(\Delta_+ \frac{\tanh\frac{1}{2}\beta E_+}{2E_+} + \Delta_- \frac{\tanh\frac{1}{2}\beta E_-}{2E_-} \right),$$
(1a)

$$\Delta_+ - \Delta_- = -\sum_{\mathbf{q}} V_\perp \left(\Delta_+ \frac{\tanh\frac{1}{2}\beta E_+}{2E_+} - \Delta_- \frac{\tanh\frac{1}{2}\beta E_-}{2E_-} \right),$$
(1b)

where we define

$$E_\pm^2 = \epsilon_\pm^2 + |\Delta_\pm|^2. \tag{2}$$

Here we make the reasonable assumption that weak coupling theory is adequate for indicating the form of the order parameter, although not for giving a reliable magnitude of T_c. Equation (1) was previously discussed in Ref. 8. Its general derivation is presented in the N-layer context in Sec. III A. The two order parameter components Δ_+ and Δ_- refer to pairing on the bonding and antibonding bands of the Fermi surface, respectively. Throughout this paper we will transform between the band and layer indices. The two gap parameters may be related to order parameters in the layer language by the equations

$$\Delta_+ = \Delta_\parallel + \Delta_\perp,$$
$$\Delta_- = \Delta_\parallel - \Delta_\perp, \tag{3}$$

where $\Delta_\parallel$ refers to singlet pairing of electrons within individual layers and $\Delta_\perp$ refers to singlet pairing of electrons on different layers. Finally, the normal state energy dispersion is given by $\epsilon_\pm = \xi \mp t_\perp$, where $t_\perp$ is the interlayer hopping matrix element and $\xi(\mathbf{q})$ is the single particle dispersion within the copper oxide planes. It should be noted that allowing the interlayer tunneling to depend on $\mathbf{q}$ in the manner suggested by Chakravarty and Anderson[30] as well as Andersen et al.,[42]

$$\frac{t_\perp}{4}(\cos q_x - \cos q_y)^2, \tag{4}$$

has no qualitative effect on the results of this paper. This arises because for the model of Ref. 30 the interplane tunneling deviates most from the constant value $t_\perp$ along the diagonals of the Brillouin zone [where Eq. (4) vanishes]. It is in precisely this region where the density of states contributions are smallest, since, as will be discussed in more detail below, they lie away from the four van Hove points.

As noted above, the bilayer system admits two other pairing states, an interlayer triplet state $\Delta_\perp^t$ which is odd under interchange of layer labels and a second intralayer singlet state $\Delta_\parallel^o$ where the order parameter has opposite phase on each of the two layers. Both of these correspond to interband pairing, i.e., pairing between electrons on different subbands of the Fermi surface. Thus they appear as off-diagonal elements of Δ in the band representation. Because this interband pairing is associated with a second phase transition (when $t_\perp$ is finite) as well as a triplet state, it appears to be currently of less physical interest than the singlet, intraband pairing which we consider here. For the purposes of completeness, these more exotic states are considered in Appendix B.

In order to analyze Eq. (1) we adopt a model interaction which is believed to be sufficiently generic so as to encompass most pairing mechanisms in the literature. In the spirit of weak coupling theory it contains no dynamical effects, although it includes as limiting forms the well studied spin fluctuation interaction, which is strongly peaked at quasimomentum transfers of $\mathbf{Q}=(\pi,\pi)$,[1] as well as phonon based mechanisms.[43] Alternative scenarios[44] may be associated with intermediate $\mathbf{Q}$ values. In the present model, the inplane and interplane pairing interactions are given by

$$V_\parallel(\mathbf{q},\mathbf{q}') = \lambda_\parallel \chi_{\mathbf{Q}_0}(\mathbf{q}-\mathbf{q}'),$$
$$V_\perp(\mathbf{q},\mathbf{q}') = \lambda_\perp \chi_{\mathbf{Q}_0}(\mathbf{q}-\mathbf{q}'), \tag{5}$$

where we define the generalized susceptibility, which depends on the momentum transfer

$$\chi_{\mathbf{Q}_0}(\mathbf{q}) = \frac{1}{h} \sum_{\mathbf{Q}=R\mathbf{Q}_0} \frac{1}{[1 - J_0(\cos(q_x - Q_x) + \cos(q_y - Q_y))]^2}. \tag{6}$$

This model incorporates several parametrizations, allowing the variation of the peak location through $\mathbf{Q}_0$, the peak width via J_0, and the coupling strength and sign through λ. We consider J_0 to be below the critical value 0.5. The interaction contains the underlying symmetry of the lattice. This is imposed by summing over all elements R of the point group, h being the order of the group. Thus when $\mathbf{Q}_0$ does not lie on a symmetry element of the lattice then the interaction will have eight peaks in a tetragonal D_{4h} lattice and four peaks in an orthorhombic lattice.

Our aim is to incorporate some of the key features of the known band structure in various cuprates. Thus the lattice point group will be assumed either to be D_{4h} in the case of La-Sr-Cu-O (LSCO) or D_{2h} in the case of YBCO and BSCCO. We investigate two different kinds of broken tetragonal symmetry in which either principle axes are retained as symmetry planes (orthorhombic) in the case of YBCO or the diagonals are retained as planes of symmetry (rhombohedral)[45] in the case of BSCCO.[46] The band struc-

TABLE I. Tight binding basis functions and hopping parameters (in eV) used in numerical calculations.

$\eta_i(\mathbf{q})$	t_i		
	LSCO	YBCO	BSCCO
1	0	0	0.1305
$\frac{1}{2}(\cos q_x + \cos q_y)$	-1.0	-0.50	-0.5951
$\cos q_x \cos q_y$	0.2	0.15	0.1636
$\frac{1}{2}(\cos 2q_x + \cos 2q_y)$	0	-0.05	-0.0519
$\frac{1}{2}(\cos 2q_x \cos q_y + \cos q_x \cos 2q_y)$	0	0	-0.1117
$\cos 2q_x \cos 2q_y$	0	0	0.0510
$\frac{1}{2}(\cos q_x - \cos q_y)$	0	0.04	0
$\sin q_x \sin q_y$	0	0	0.08

tures which we use throughout this paper are taken from Ref. 47. In plane energy dispersions of the normal state are given by an expansion of the form

$$\xi(\mathbf{q}) = \sum_{i=0}^{7} t_i \eta_i(\mathbf{q}), \qquad (7)$$

where the basis functions η_i are listed in Table I. Also indicated in the table are the various band structures we will be considering. It is important to note that the degree to which the tetragonal (D_{4h}) symmetry is broken is reflected in the last two parameters of the table which we call t_6 and t_7. The size of these orthorhombic contributions was chosen, for illustrative purposes, to be small, but otherwise arbitrary.

B. Order parameter symmetry in bilayers

1. Properties of monolayer solutions

Solutions to the single layer problem provide intuition into those of the N-layer case, particularly when the interlayer hopping is relatively small. It is useful, therefore, to characterize the allowed order parameters in the one layer limit for each of the three band structures discussed above, before moving to the bilayer case. In the one layer system the functional form of the superconducting order parameter depends only on the sign and the shape (as distinct from the magnitude) of the pair interaction and on the electronic structure. To illustrate these pair interaction and electronic effects, we vary the position of the peak location $\mathbf{Q}$ and plot the associated form of the order parameter in this two dimensional space, for each of three model band structures. The interaction is assumed repulsive ($\lambda > 0$) in this and subsequent phase plots; attractive interactions in general give rise to nodeless s-wave solutions for any value of $\mathbf{Q}$. The magnitude of the interaction plays no role in determining the symmetry of the order parameter in the single layer problem, it results only in a variation of the transition temperature. By contrast, in the two layer case the (relative) magnitudes of the in plane and out of plane interactions enter via Eq. (1) in an important way. We will examine this effect subsequently.

Other parameters of our model interaction have a lesser influence on the form and regions of stability of the various solutions. Variation of the peak width J_0 affects T_c to a greater extent than it does the symmetry of the actual solution. The component of the interaction which most influences
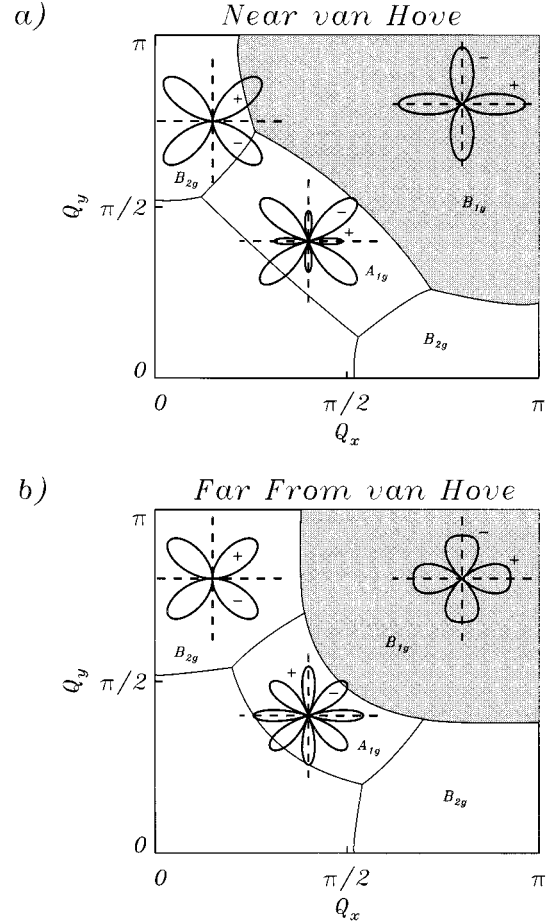

FIG. 1. Phase diagram showing order parameter symmetry in LSCO: (a) near van Hove points; (b) away from van Hove points. The two axes represent the wave vector components Q_x, Q_y at which the pairing interaction has a maximum.

the symmetry of the superconducting order parameter is the degree to which the vector $\mathbf{Q}$ connects positive and negative lobes of the pair wave function on the Fermi surface.[37] As will be illustrated under more general circumstances below, near half filling, when only nearest neighbor hopping is included, the points at which the $d_{x^2-y^2}$ state has maxima are separated by $\mathbf{Q} = (\pi, \pi)$, while the extrema of d_{xy} are separated by $(\pi, 0)$ and the eight lobed s_{xy} state has positive and negative lobes separated by $(\pi/2, \pi/2)$. These are precisely the points in the space of $\mathbf{Q}$ near which these various solutions are favored.

Figure 1 represents this "phase diagram" for the LSCO case. It is a map of the irreducible representations of the tetragonal, D_{4h} lattice which correspond to the solutions with the highest T_c. We stress that the simple functional forms of the order parameter, such as are implicit in the notation "$d_{x^2-y^2}$" etc., can be misleading. The gap parameters may involve important contributions from higher order terms in the associated representation. Moreover, when tetragonal symmetry is broken, states may be highly admixed with states of other representations. We will use this notation with care, applying it only to certain solutions of systems with tetragonal symmetry. When necessary we will avoid any am-

biguity by using the common group theoretic nomenclature for the various irreducible representations.[48]

Because proximity to the van Hove singularity is found to play such a crucial role, we present two limiting cases corresponding to choices for the Fermi energy near 1(a) and far from 1(b) the van Hove singularity. The order parameters shown plot the actual solutions for $\mathbf{Q}=(\pi,\pi)$, at which the B_{1g} ("$d_{x^2-y^2}$") solution is found, at $\mathbf{Q}=(\pi/2,\pi/2)$, where an eight-lobed A_{1g} solution, the so called "s_{xy}" state, exists and at $\mathbf{Q}=(\pi,0)$, where the B_{2g} "d_{xy}" state is most stable. Moreover, these symmetries persist over an extended region of $\mathbf{Q}$ space as outlined by the solid lines in the figures. States with increasing numbers of nodal planes, including states in the A_{2g} irreducible representation, appear as $\mathbf{Q}\rightarrow(0,0)$. Indeed, because this region is so complicated (in the case of repulsive interactions), no detailed solutions are indicated. The region where the "$d_{x^2-y^2}$"-like solution persists is shaded in this and subsequent figures.

Figures 1(a) and 1(b) demonstrate that proximity to the van Hove singularity leads to a modestly extended region with B_{1g} or "$d_{x^2-y^2}$" symmetry. Moreover, as the Fermi energy approaches the singularity, the lobes on the "$d_{x^2-y^2}$" state become sharper. In this way the order parameter takes full advantage of the four van Hove points which coincide with each of the four maxima in this gap function. Since the gap function is sharply peaked in the direction of the principle axes it is very small in a large region about the nodal lines along the diagonals of the Brillouin zone. A large gapless region will have consequences on the thermodynamic properties of the samples at low temperatures and may have been observed in angle-resolved photoemission spectroscopy measurements on BSCCO.[4,5]

Breaking of the tetragonal symmetry in our model band structure, as is appropriate for orthorhombic YBCO, serves to further enhance these van Hove effects. This is shown in Fig. 2 where, as in the LSCO case above, the gap equation solutions are plotted at the special symmetry points and the lines indicate the boundaries of the region over which the representative solution persists. Solid lines separate states belonging to different irreducible representations and dotted lines separate states of different symmetry within a representation. Figures 2(a) and 2(b) demonstrate clearly that the phase space occupied by the "$d_{x^2-y^2}$" solution is dramatically increased in the vicinity of the van Hove point. Furthermore, the lobes of this gap function again become more extended along the principle axes, compared with similar solutions farther from the van Hove point.

Finally, the results in the BSCCO case are presented in Fig. 3. We see here that, contrary to the two previous cases, the phase space in which the gap has the same sign along the a and b directions (i.e., the totally symmetric irreducible representation in the D_{2h} lattice) occupies a somewhat larger region of parameter space when the Fermi level is near the van Hove point. This is the consequence of a stabilizing admixture of an isotropic s-wave component. On the other hand, states with an a,b-axis π phase shift dominate the phase space away from the van Hove points.

The above three figures lead to an important conclusion: the "$d_{x^2-y^2}$" solution exists in a large region of parameter space away from $\mathbf{Q}_{AF}$. Therefore this state should be considered as an obvious candidate form for the order parameter
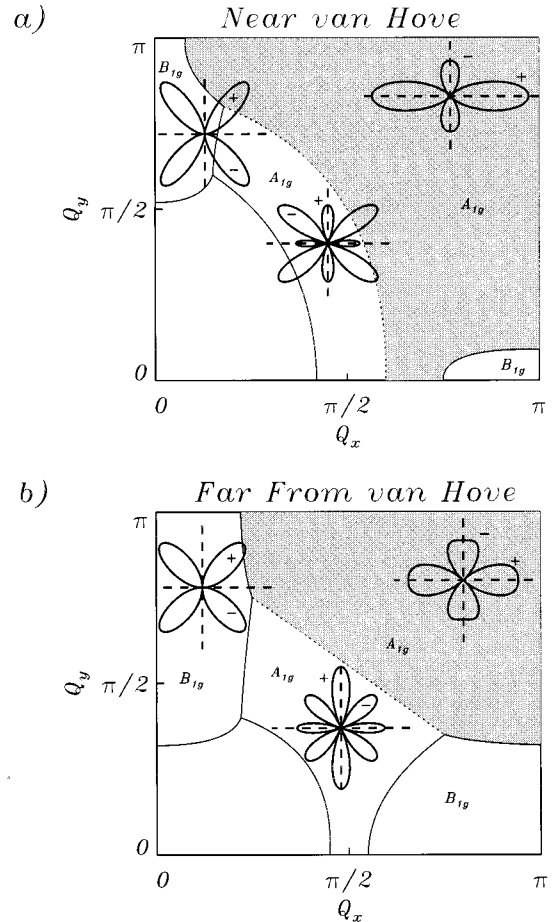

FIG. 2. Phase diagram for one layer model of YBCO: (a) near van Hove points; (b) away from van Hove points. The dotted line separates A_{1g} representations with and without a,b-axis π phase shifts.

in any mechanism involving pairing via a predominantly repulsive interaction. Stated alternatively, observation of this form for the gap in an experiment is in itself not proof of any specific pairing mechanism. Furthermore, it also appears from these figures that, quite frequently, a single mechanism can give rise to widely varying forms of order parameters depending upon the details of the band structure, doping level, lattice symmetry and other subtle features of the material.

2. Bilayer effects

In bilayer materials there are two possible states which compete as solutions to the gap equation. These may be crudely classified by referring to the states as "interplane and intraplane dominated solutions." These two competing sets of solutions were discussed in a previous short communication by our group,[8] as well as elsewhere.[9,11,22,49] By setting $t_\perp=0$ in the gap Eq. (1) we see that $\Delta_\parallel$ and $\Delta_\perp$ uncouple from each other at T_c. Superconductivity can thus be either due to interlayer pairing or due to intralayer pairing depending on the relative magnitudes and signs of $\lambda_\parallel$ and $\lambda_\perp$. In the band representation in-plane pairing yields a solution which
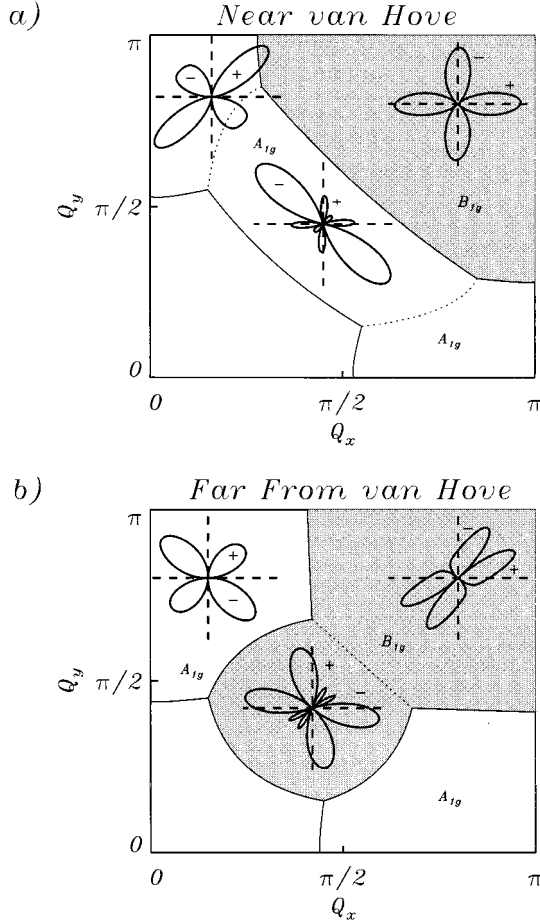
FIG. 3. Phase diagram for one layer model of BSCCO: (a) near van Hove points; (b) away from van Hove points. A dotted line separates states with four and eight lobes within a representation.

FIG. 4. Phase diagram for stability of π phase shifts on the a relative to the b axis, in the order parameter (below solid line). Model is for YBCO with an attractive interlayer and repulsive intralayer interaction, both peaked at $\mathbf{Q}_{AF}$. Hole doping fraction appears on the ordinate and relative strength of the two interactions defines the abscissa. The shaded regions denote states where the order parameter on one (light) or both (dark) bands is nodeless.

has the same phase on both bands while the interlayer pairing solution undergoes a π change in phase from one band to the other. This sign change follows directly from Eq. (3) in the extreme limits in which one or the other order parameter (in the layer basis) is the larger.

It is important to stress that we will refer to these two competing solutions throughout this paper. They occur in bilayer as well as N-layer systems. In all cases where $t_\perp$ is finite, one solution is stable and the other metastable. Thus, although one may refer to their associated transition temperatures, only the larger of the two has any physical meaning. As a consequence, there is nothing to prevent these two competing states from having a different order parameter symmetry.

As in the one layer case, repulsive interactions are found to lead to nodal states such as the d states or multilobed s states discussed above, while attractive interactions require nodeless states of s symmetry. In the presence of two different types (signs) of in plane and out of plane interactions, these effects provide a rich and complex structure for the competing order parameter states. Under these conditions and when there is no coherent interplane hopping, the two solutions may belong to different symmetry groups. When $t_\perp$ is finite, the solutions couple while still preserving the
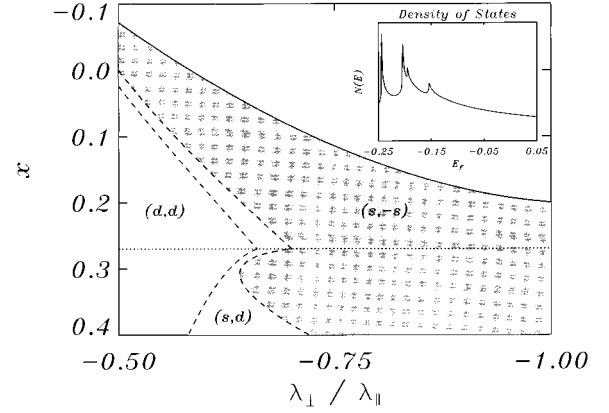
underlying lattice symmetry. Thus mixing of s and d states within the linearized gap requires both orthorhombicity and interplane hopping. More general s-d mixing effects will occur at higher (quartic) order in a Landau-Ginzburg expansion, and will be discussed in more detail in a subsequent section.

To illustrate the behavior of the bilayer order parameter and the two competitive states, we consider for concreteness the case of an attractive interplane interaction and a repulsive intraplane interaction peaked at $\mathbf{Q}=(\pi,\pi)$. This model may be viewed as derived from a generalized spin fluctuation model, where the interlayer or c-axis spin susceptibility is included as a perpendicular component of the pairing interaction. This case was previously discussed by a number of different groups.[8,9,11,20,49,50] While we choose this peak location simply for illustrative reasons, our results can easily be extended to other values of $\mathbf{Q}$. Under these circumstances, the order parameter in the band picture has the schematic form

$$\begin{pmatrix} \Delta_+ \\ \Delta_- \end{pmatrix} = \begin{pmatrix} s_\perp + d_\parallel \\ -s_\perp + d_\parallel \end{pmatrix}. \qquad (8)$$

If the lattice is tetragonal then either $s_\perp$ or $d_\parallel$ will vanish. Thus when $\lambda_\perp$ is zero the solution will have d symmetry. Moreover, both band gaps are in phase. Similarly when $\lambda_\parallel$ vanishes the symmetry is s-like and both gaps are out of phase. The transition from one type of solution to the other is governed by the size of $\lambda_\perp/\lambda_\parallel$. Frequently the crossover from the in-plane to the interplane dominated regime may occur despite the fact that the ratio $\lambda_\perp/\lambda_\parallel$ is small compared to one. What determines this crossover is the nature and sign of the competing interactions and the band structure.

If tetragonal symmetry is broken even more complicated situations obtain. Both components can be nonzero simultaneously and the transition is a smooth one as a function of increasing $\lambda_\perp/\lambda_\parallel$. The regions where the various types of solution exist in YBCO are illustrated in Fig. 4 for the ex-
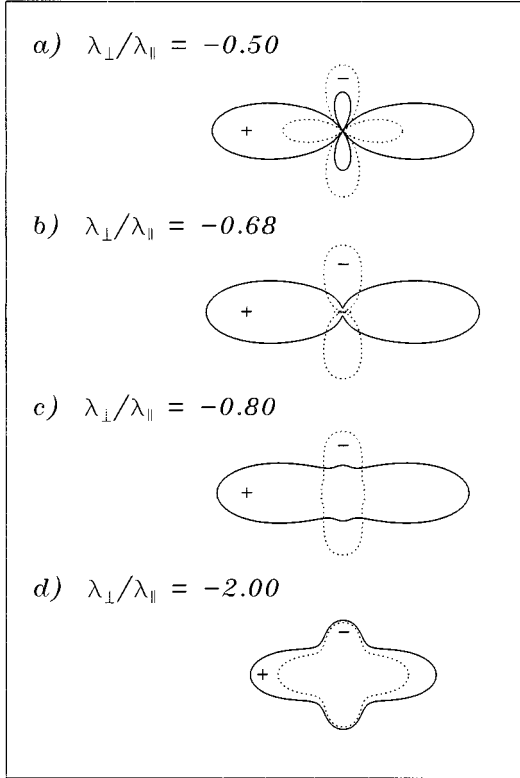
FIG. 5. Evolution of order parameter solutions as interlayer correlations are increased. The states correspond to the solutions obtained in the previous figure for $x=0.25$ and the indicated $\lambda_\perp/\lambda_\parallel$. Observe that proximity to the van Hove singularity results in considerable a,b-axis anisotropy despite the very small orthorhombicity.

ample discussed above. Plotted on the vertical axis is the fractional hole doping x. We estimate the physical values of this parameter, for a range of different oxygen stoichiometries in YBCO, to vary from 0.1 to 0.3. The figure illustrates the parameter regimes where the dominant component of the order parameter on the two bands is (d,d),(s,d), and $(s,-s)$.[51] The region below the solid line involves states in which the sum of the pair wave functions on the two bands changes sign under $\pi/2$ rotation of the axes and can thus yield π phase shifts in a,b-axis Josephson tunneling experiments.[14–17] Moreover, the shaded regions denote states in which the sum of the two order parameters changes sign even though one or both are nodeless. This issue will be addressed in detail in Sec. II C. The inset plots the density of states as a function of energy. There are actually four van Hove points associated with orthorhombic splitting of the two bands. For clarity the doping level at which the first of these occurs is plotted in the main portion of the figure as a dotted line. Note that the region labeled by $(s,-s)$ occupies the largest fraction of phase space when the band is near the van Hove points in general and in particular when one subband of the Fermi level is closed about the Γ point of the reciprocal lattice and the other about X.

The evolution of these solutions with increasing $\lambda_\perp/\lambda_\parallel$ is illustrated in Fig. 5. Indicated here is the calculated shape of the gap functions for the two bands of the bilayer. Their relative phase is also noted. It can be seen that the pair wave

function on each band has a greater amplitude along one symmetry axis than along the other, and the axis along which the pair wave function has its maximum differs from one subband to the other. These results are plotted for very small orthorhombicity and for Fermi energies close to the van Hove point. On the basis of the latter assumption, the small orthorhombic effects are greatly magnified. The figure labels (a)–(d) correspond to (a) two in phase d-wave dominated states, (b) one band nodeless and the other nodal, (c) two out of phase nodeless states which show greatly elongated lobes, and (d) to two out of phase s-wave dominated states which are more isotropic. The relative phase space which these solutions occupy can be seen from the previous figure.

Moreover, the detailed shape of the order parameter has important physical consequences. Thus for case (c), for example, the solutions are in the interplane regime where $\Delta_\perp$ is dominant. Here, however, the order parameter is nodeless and yet the combination of the two gaps has features of a d-wave solution in a,b-axis as well as c-axis Josephson tunneling experiments.[52] Case (b) is associated with one s-like and one d-like state. It will exhibit both power law behavior in thermodynamical properties, as well as the π phase shifts in corner junction experiments, which are also seen in cases (a) and (c). These Josephson experiments and their relation to the order parameter symmetry will be discussed in more detail in the next section.

C. Josephson tunneling: Phase coherence across domain boundaries

Josephson tunneling experiments have been key to elucidating the order parameter symmetry in the YBCO cuprate family.[14–17,52] Within this class, two types of measurements have been performed. These involve a,b- and c-axis tunnel junctions. In the former category superconducting quantum interference device (SQUID) geometries have been investigated.[15–17] These consist of two junctions with Pb counterelectrodes, whose interference pattern yields information about the relative phase of the order parameter along various axes in the a,b plane. In "corner junctions," π phase shifts of the order parameter between the a and b axes have been observed and attributed to the sign change upon a $\pi/2$ rotation of the wave vector, within a $d_{x^2-y^2}$ state. This interpretation is further confirmed by "edge" junctions which probe the interference along a single face of the material; here no phase shifts are found to be present. These conclusions are the same for both twinned and untwinned crystals. A variant on this geometry are the ring experiments[14] consisting of YBCO segments with different grain boundary orientations. Observation of a nonzero, half integer spontaneous flux threading the ring, for specific orientations of the grain boundaries, again provides support for a $d_{x^2-y^2}$ state.

An alternate Josephson tunneling geometry has been investigated by Sun $et\ al.$[52] These authors observe finite c-axis Josephson currents between a Pb counterelectrode and a YBCO sample. For the simplest representation of the $d_{x^2-y^2}$ symmetry, no Josephson current should be present. While it is possible to invoke orthorhombicity[52,53] to explain these nonvanishing results, this hypothesis has been chal-

lenged since the presence of the current is evidently not sensitive to the averaging over domains which results when twins are present.

To the extent that twinned YBCO can be treated as a tetragonal system, these two types of experiments appear manifestly incompatible. π phase shifts are associated with a sign change of the order parameter in the a,b plane. The c-axis current, which reflects an average of the order parameter in the a,b plane, must necessarily vanish. These observations are not altered when bilayer effects are incorporated. While there has been some attention[23-25] paid to the role of chains in addressing the data, it should be noted that recent experiments on reduced oxygen YBCO (Ref. 15) (where the chains are expected to be highly interrupted and, therefore, irrelevant to the transport and superconductivity), seem to reproduce the same behavior as in the optimally doped material. In summary, if both a,b- and c-axis Josephson measurements prove to be correct, any resolution of this issue will probably revolve around a deeper understanding of twinning effects.

In a Josephson experiment, the measured Josephson current is the sum of the currents established between each band of the cuprate and the superconductor to which it is coupled

$$J = J^+ + J^-, \qquad (9)$$

where each component has the usual Ambegaokar-Baratoff form[54]

$$J^{\pm} = \Delta_{\pm}^L \Delta^R \frac{\pi}{\beta r_{\pm}} \sum_n \left[(\omega_n^2 + \Delta_{\pm}^{L\,2})(\omega_n^2 + \Delta^{R2}) \right]^{-1/2}. \qquad (10)$$

The resistances, $r_{\pm}$, can be calculated by determining the single particle tunneling matrix elements[55]

$$T_{k,k'}^{\pm} = \int dr \langle \phi_{k,\pm}^L | j(r) | \phi_{k'}^R \rangle, \qquad (11)$$

where the integration is carried out over the intermediate region of the junction. The wave functions $\phi_{\pm}^L$ and ϕ^R are the single particle wave functions from the left and right hand side of the junction, respectively, and $j(r)$ is the usual current operator. The fact that the electrons of the cuprates are localized on the copper-oxide planes requires that they be described by wave packets with some finite spread in momentum along the c-axis direction. A microscopic treatment of the tunneling process is complicated by a number of issues, which we cannot address here: the propagation of electrons out of a region of localization in the c direction will lead to scattering effects as the tunneling pair enters a more isotropic material. These may influence the tunneling from both bands to a substantial degree. (It should also be noted that the order parameter at the surface may be modified from its bulk form.[56]) For definiteness, we first consider the case of coupling to a conventional superconductor such as Pb, and ignore these complications.

If we make the simplifying assumption that the Josephson coupling is the same for both the symmetric (+) and antisymmetric (−) bands, it follows that π phase shifts in a SQUID experiment will be observed in a substantial region of the phase space, corresponding to all bilayer parameter sets which lie below the solid line of Fig. 4. Moreover, for a
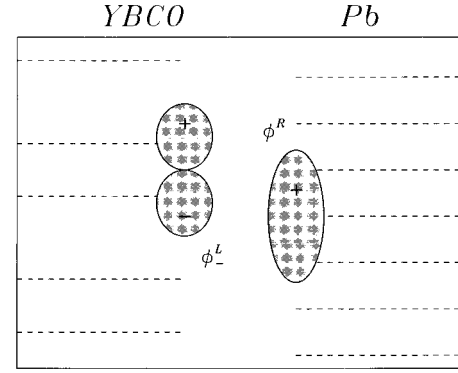

FIG. 6. Schematic illustration of Josephson coupling between the antibonding band in YBCO (left) and a Pb counterelectrode (right). Overlap of the single particle wave functions is nonzero unless the two wave functions are perfectly aligned in the directions parallel to the plane of the interface.

significant fraction of these (particularly in the vicinity of the van Hove points), the states in question differ from two in phase d-like states. They are described by (s,d) or $(s,-s)$ dominant combinations. In this way, the measurement of π phase shifts cannot be uniquely associated with d states in a multilayer system, provided orthorhombicity is also present. From the standpoint of determining the order parameter symmetry the most decisive experiments would, therefore, be performed on monolayer, tetragonal systems. Recently we learned of the observation of a π phase shift by Tsuei and co-workers[57] in a one-layer, tetragonal Tl compound. This provides the most persuasive evidence for d-wave pairing, presumably due to a repulsive in-plane interaction in these materials.

In reality, there is some asymmetry in the Josephson coupling to the symmetric and antisymmetric bands. This asymmetry derives from (1) density of states effects related to the van Hove points, and (2) single particle wave-function structure: wave functions associated with the antibonding band of the bilayer cuprate have opposite phase on the two layers and therefore a nodal plane exists between the layers. The first effect indirectly favors tunneling from the bonding band, although its importance is strongly dependent on the magnitude of the bilayer splitting. In most of the high-T_c cuprates for which band structure data are available, the Fermi surfaces are closed about the (π,π) point so that the antibonding band lies closer to the van Hove points and thus has a higher density of states. The effects of this higher density of states are manifested via the gap magnitudes: $|\Delta_+| > |\Delta_-|$.[58]

On the other hand, the second effect, although also favoring tunnelling from the bonding band, is much less important. It has been claimed[59] on the basis of symmetry arguments that tunnelling from the antibonding band into an s-wave superconductor will lead to an appreciable reduction in the current contribution from this band. However, some Josephson coupling is expected to remain; the matrix elements $T_{k,k'}^-$ only vanish under special circumstances, when the centers of the two wave functions of Eq. (11) coincide throughout the boundary region. In general, this matrix element will be nonzero, if for no other reason than because the
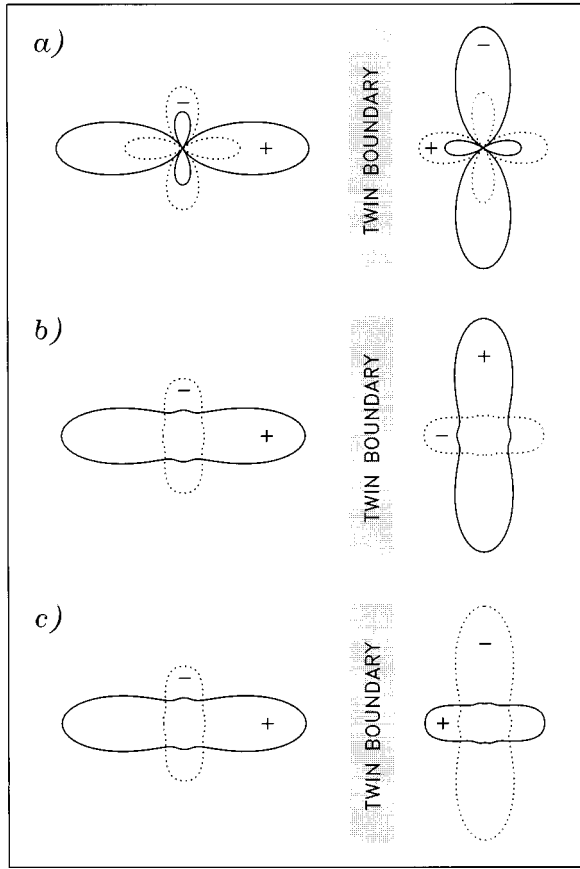
FIG. 7. Possible scenarios for order parameter behavior across twin boundaries showing π phase shifted (d,d)-type (a) or $(s,-s)$-type [(b) and (c)] solutions. The scenarios depicted in (a) and (c) give π junction behavior in a,b-axis corner junctions while case (b) will lead to cancellation of the π phase shift after averaging over twin domains.

lattice constants of the two materials are unlikely to be commensurate. The situation is depicted in Fig. 6.

The net result is that the contribution to the tunnelling current from the bonding band is somewhat greater than that from the antibonding band but both bands contribute in an important way.[23] It thus becomes clear that the possibility of π phase shifts due to a nodeless order parameter must be seriously considered when interpreting SQUID experiments on orthorhombic multilayer materials.

Josephson tunneling from one YBCO crystal to another, as well as across twin boundaries, is even less amenable to microscopic theory. In many respects twinned materials behave like single crystals, with similar transition temperatures, thermodynamics and Josephson currents in corner and c-axis junctions. It is clear that little is understood at a detailed theoretical level about the nature of the twin boundary. What seems to be less ambiguous, however, is that there is little if any pinning of the critical current (in low magnetic fields) as it flows between twin boundaries.[60] This would suggest that, whatever the order parameter symmetry, the phases tend to line up with + and − lobes along parallel directions in different domains.

In the context of a bilayer system, this situation is more complex, since the phases are associated with multiple bands. In Fig. 7, we schematically plot the two alternative scenarios for the $(s,-s)$ (orthorhombic) bands [parts (b) and (c)], as well as the generally expected behavior for the (d,d) case (a). Of the two scenarios (b) and (c), only the latter would preserve the π phase shift behavior across a twin boundary. This scenario would also be compatible with a low twin boundary pinning of the critical current. On the other hand only case (b) would unambiguously lead to a finite c-axis Josephson current. Moreover, neither case can be ruled out on microscopic grounds.

In the extreme limit where the boundary can be treated as a conventional superconductor-insulator-superconductor (SIS) junction, the locking of the phase of the order parameter across the junction occurs via Josephson coupling. If the bilayers on either side of the junction are properly aligned it might be expected that only bands of equal symmetry couple together since the matrix element in Eq. (11) vanishes otherwise. Thus the even bands on either side of the junction would couple together as would the odd bands. As a consequence the positive lobes of a $(\Delta_+,\Delta_-)=(d,d)$ solution would point in the same spatial direction on both sides of the twin boundary [scenario (a)]. On the other hand the $(s,-s)$ state would have the component of positive phase in one twin aligned with the component with negative phase in the other twin [scenario (b)]. This would lead to a substantially reduced Josephson current at a macroscopic junction due to averaging over the twins. If instead of an SIS model, one argued that the order parameter lobes were required to vary in the most continuous fashion, one might conclude that the dominant component $\Delta_\perp$ should also be continuous. This, too, would lead to scenario (b) for the $(s,-s)$ states and (a) for the (d,d) configuration.

Nevertheless, it is also possible to assume that interlayer pair breaking effects become considerable in the boundary region and that $\Delta_\parallel$ retains its coherence between twins so that scenario (c) obtains. Moreover, stacking faults, lattice defects and other complexities can invalidate any of the above simple models of twinned crystals. In summary, the nature of the order parameter variation across a twin boundary is quite complicated in one layer systems and sufficiently complex in the bilayer case so that no clear conclusions can be drawn at this time.

D. Landau-Ginzburg free energy functional

Thus far we have investigated only the linearized gap equations, which are necessarily restricted to the vicinity of the transition temperature. Additional effects may occur below T_c associated with the transition to states with other order parameter symmetries. While there does not appear to be experimental evidence for additional phase transitions, there is considerable information contained in studying the more general situation. In this section we derive the appropriate Landau-Ginzburg free energy functional in terms of both the layer and band indices. The behavior at quadratic order gives further insight into, and serves to validate the results discussed in the previous sections. There have been several discussions in the literature[22,44] of phenomenological forms for the bilayer free energy. Here we proceed from a microscopic basis. Note that while this discussion refers to a bilayer structure, it is readily extended to the case of general N following the results of Sec. III B.

In the case under consideration (when only pairing of electrons on individual subbands of the Fermi surface is considered), the superconducting state of the bilayer is described by a two component order parameter : Δ_+ and Δ_- . The free energy, F_s, of the superconducting state then consists of the sum of terms

$$F_s = F_{s,+} + F_{s,-} , \tag{12}$$

where $F_{s,\pm}$ is the contribution to the free energy of an individual subband. In the Landau-Ginzburg limit the free energy difference between the normal and superconducting states is given by

$$F_{s,\pm} - F_{n,\pm} = \ln\frac{T}{T_c} \int_{\epsilon_\pm = E_F} \frac{dS}{(2\pi)^2 v_F} |\Delta_\pm|^2 + \frac{0.0533}{(k_B T_c)^2} \int_{\epsilon_\pm = E_F} \frac{dS}{(2\pi)^2 v_F} |\Delta_\pm|^4 . \tag{13}$$

It should be stressed that, although the two subbands contribute independently to the free energy, the two order parameters are coupled via the gap equation. Both become finite at a common T_c.

By use of the gap equations the Landau-Ginzburg free energy functional can be recast into a form which contains a quadratic part,

$$\alpha_+ |\Delta_+|^2 + \alpha_- |\Delta_-|^2 + \delta(\Delta_+ \Delta_-^* + \text{c.c.}), \tag{14}$$

and a quartic contribution,

$$\beta_+ |\Delta_+|^4 + \beta_- |\Delta_-|^4$$
$$+ (\Delta_+ \Delta_-^* + \text{c.c.})(\mu_+ |\Delta_+|^2 + \mu_- |\Delta_-|^2). \tag{15}$$

Here we have assumed that each component of the order parameter can be separated into a complex magnitude times a normalized real function over the Fermi surface:

$$\Delta_\pm(\mathbf{q}) = \Delta_\pm \psi_\pm(\mathbf{q}). \tag{16}$$

The magnitude $\Delta_\pm$ appears explicitly in the Landau-Ginzburg free energy expansion while $\psi_\pm$ determines the coefficients in the expansion. The coefficients δ and $\mu_\pm$ vanish if Δ_+ and Δ_- belong to different irreducible representations of the lattice point group.

These coefficients have been discussed by Varma in the context of a particular pairing scenario.[44] While our free energy contains the same class of terms as that presented in Ref. 44, because we have explicitly removed the wave vector dependences via Eq. (16) above, it is not straightforward to determine the conditions for order parameter sign changes under a $\pi/2$ rotation of the lattice. Nevertheless, the relative phase of the two order parameters can be determined variationally, by minimizing the free energy. If the nontrivial coupling parameters (δ and $\mu_\pm$) are finite then the phase difference between Δ_+ and Δ_- can be at most 0 or π. This last result is consistent with the discussion of Sec. II B 2 and the appropriate sign depends on whether in-plane or interplane correlations are dominant.[61]

It is useful to transform the above free energy functional to the layer representation using Eq. (3). The functional is expressed in terms of $\Delta_\parallel$ and $\Delta_\perp$ and two explicit transition temperatures can then be associated with the intra- and interplane interactions. In this context the mixing between various symmetries can be understood in a more direct way. In this representation the free energy is given by[62]

$$\alpha_\parallel |\Delta_\parallel|^2 + \alpha_\perp |\Delta_\perp|^2 + \delta'(\Delta_\parallel \Delta_\perp^* + \text{c.c.}) + \beta_\parallel |\Delta_\parallel|^4 + \beta_\perp |\Delta_\perp|^4$$

$$+ \beta' |\Delta_\parallel|^2 |\Delta_\perp|^2 + \gamma'(\Delta_\parallel^2 \Delta_\perp^{*2} + \text{c.c.})$$

$$+ (\Delta_\parallel \Delta_\perp^* + \text{c.c.})(\mu_\parallel |\Delta_\parallel|^2 + \mu_\perp |\Delta_\perp|^2). \tag{17}$$

Here the coupling terms δ' and $\mu_{\parallel/\perp}$ vanish if $\Delta_\parallel$ and $\Delta_\perp$ belong to different irreducible representations of the lattice symmetry group. Note that one important effect of orthorhombicity is to require that the coupling parameters δ' and $\mu_{\parallel/\perp}$ change sign upon the interchange of the a and b axes of the crystal. These same terms also vanish in the limit as $t_\perp$ goes to zero.

By direct calculation from the microscopic theory we find that the quartic cross term γ' is positive[63] so that the phase difference between $\Delta_\parallel$ and $\Delta_\perp$ is zero (if $\delta' < 0$) or π (if $\delta' > 0$).[64] Studies of a related Landau-Ginzburg free energy functional have been presented by Kobuki and Lee[22] who discussed the mixing between a d-wave $\Delta_\parallel$ and an s-wave $\Delta_\perp$ in an RVB based theory. In their approach, mixing between these two components was brought about by a self-consistently determined orthorhombic strain. This led to the introduction of additional terms into the free energy which could result in a negative γ'. As a consequence an $s + \iota d$ state was produced. In the present theory, in contrast, mixing between $\Delta_\perp$ and $\Delta_\parallel$ occurs at quadratic rather than quartic order, as a consequence of finite $t_\perp$. Furthermore, in the absence of tetragonal symmetry breaking only $s + d$ mixing occurs (at quartic order). Additional arguments against an $s + \iota d$ state were presented by Normand *et al.*[50]

E. Impurity effects

In this section we discuss the nature of impurity or pair-breaking effects in bilayer systems. At the heart of this issue is the paradoxical observation that all substitutions at the rare earth site, which sits between the bilayers (except for Pr), leave T_c unaffected. Rare earth substitutions with or without local moments and in a disordered or ordered form make no difference to the superconducting transition temperature. Previously it has been argued that the even more general insensitivity of the cuprates to impurity substitution is incompatible with anisotropic or d-wave superconductivity.[38–41] Here we investigate the complexity introduced into this problem by the presence of a bilayer order parameter. The effects of both magnetic and nonmag-

netic impurities on two-band systems have been considered in Ref. 20. Since it is relatively straightforward to generalize to the magnetic case, for definiteness, we concentrate on the case of nonmagnetic impurities.

A central aspect of the present work is the consideration of an isolated bilayer, rather than a coherent stack of bilayers. Our starting point is a necessary first step in a treatment of incoherent coupling along the c axis. As a result of this assumption the configuration averaging process (which restores the underlying translational symmetry of the lattice) is different from that discussed in Refs. 13,65. As has been noted elsewhere,[13] there are two types of impurities which must be considered: intra and interlayer substitutions. For an isolated bilayer, interlayer impurities represent the more interesting case, since they result in only intraband scattering. A state such as an isotropic $(s,-s)$ state will thus be insensitive to interlayer impurities [as will the in-phase (s,s) state].[20] By contrast, intralayer impurity effects involve processes which couple the two bands. In this way, the $(s,-s)$ state exhibits intralayer pair breaking.[13] Moreover, the same concerns that were raised earlier[39,41] about the d-wave order parameter apply to the bilayer case with either type of impurity. Thus the $(s,-s)$ state emerges as the leading (nontrivial) candidate state for resolving the paradox concerning rare earth (nonmagnetic) substitutions in the cuprates.

We begin with the standard treatment of scatterers within individual planes using the Born approximation.[66] The impurity Hamiltonian has the form

$$\hat{H}_{\text{in-plane}}^{\text{imp}} = \sum_m \sum_{\mathbf{q},\sigma} u_I(\mathbf{q}) c_{i_m,\sigma}^\dagger(\mathbf{p}+\mathbf{q}) c_{i_m,\sigma}(\mathbf{p}) e^{-\iota\mathbf{q}\cdot\mathbf{R}_m},$$

(18)

where m labels impurities located at $\mathbf{R}_m$ on layer i_m and σ is a spin index. The impurity self-energy is given by

$$\Sigma_{\omega,r,r'}(\mathbf{p}) = -\frac{1}{2} n_{\text{imp}} \sum_{r'',\mathbf{q}} |u_I(\mathbf{p}-\mathbf{q})|^2 \bar{\mathscr{G}}_{\omega,r''}(\mathbf{p}) \delta_{r,r'},$$

(19)

where $\bar{\mathscr{G}}$ is the averaged Green's function and n_{imp} the concentration of impurities per layer. We assume that the gap in the absence of impurities is given by $\Delta_\pm(\mathbf{q}) = \bar{\Delta}_\pm \psi_\pm(\mathbf{q})$ where $\psi_\pm$ are functions normalized appropriately over the corresponding subband of the Fermi surface and that the impurity renormalized gap is given by $\tilde{\Delta}_\pm \psi_\pm(\mathbf{q})$. The self-consistent equations then become

$$\tilde{\omega}_l = \omega_l + \frac{1}{4\tau} \sum_{r'=\pm} \frac{\tilde{\omega}_l}{\sqrt{\tilde{\omega}_l^2 + \tilde{\Delta}_{r'}^2}},$$

(20a)

$$\tilde{\Delta}_\pm = \bar{\Delta}_\pm + \frac{g}{4\tau} \sum_{r'=\pm} \frac{\tilde{\Delta}_{r'}}{\sqrt{\tilde{\omega}_l^2 + \tilde{\Delta}_{r'}^2}},$$

(20b)

where τ is the usual scattering time and

$$\frac{g}{2\pi\tau} = \sum_{r=\pm} \sum_{r'=\pm} \int \frac{dS_r}{(2\pi)^2 v_F^r} \int \frac{dS_{r'}}{(2\pi)^2 v_F^{r'}} \times u_I^2(\mathbf{p}-\mathbf{p}') \psi_r(\mathbf{p}) \psi_{r'}(\mathbf{p}').$$

(21)

Here g is a combined measure of the anistropy of the order parameter[38] and impurity potential. This coupling constant varies from 0 to 1. The latter is appropriate to the case of a totally isotropic order parameter.

It follows from Eqs. (20) that intralayer impurities enter the coupled self-consistent equations via a mixture of the two band contributions. In this way they lead to pair breaking in all instances, except for the special case of two in phase, isotropic s states. Thus the $(s,-s)$ states experience a reduced T_c in the presence of these impurities.[67]

We next consider interplane scatterers. For the sake of generality these impurities are assumed to scatter electrons within as well as between planes. The impurity Hamiltonian is given by

$$\hat{H}_{\text{interplane}}^{\text{imp}} = \sum_m \sum_{\mathbf{q},\sigma} [u_\parallel(c_{1,\sigma}^\dagger c_{1,\sigma} + c_{2,\sigma}^\dagger c_{2,\sigma}) + u_\perp(c_{1,\sigma}^\dagger c_{2,\sigma} + \text{c.c.})] e^{-\iota\mathbf{q}\cdot\mathbf{R}_m}.$$

(22)

It is important to note that this Hamiltonian is diagonal in the band language and that no average is taken over sites in the vertical direction. Thus the renormalized self-energy and order parameter satisfy equations which are decoupled in the band index

$$\tilde{\omega}_{l,\pm} = \omega_l + \frac{1}{2\tau_\pm} \frac{\tilde{\omega}_{l,\pm}}{\sqrt{\tilde{\omega}_{l,\pm}^2 + \tilde{\Delta}_\pm^2}},$$

(23a)

$$\tilde{\Delta}_\pm = \bar{\Delta}_\pm + \frac{g_\pm}{2\tau_\pm} \frac{\tilde{\Delta}_\pm}{\sqrt{\tilde{\omega}_{l,\pm}^2 + \tilde{\Delta}_\pm^2}}.$$

(23b)

Here care must be taken to preserve the band labels on τ and g. This decoupling of the two bands leads to the conclusion, stated earlier, that isotropic order parameter sets (whether in or out of phase) experience no pair breaking from interlayer impurities.[68]

In summary, we see that one way of avoiding the strong pair breaking generally associated with substitutions at the rare earth site between the bilayers is to consider states with the symmetry $(s,-s)$. For this reason, along with the π junction behavior discussed in the previous section, this state should be considered as a potentially interesting candidate for the YBCO system.

III. FORMULATION AND ANALYSIS OF THE N-LAYER PROBLEM

A. Gap equation in the band representation

In this section, we treat the general N-layer problem. The system under consideration corresponds to a stack of decoupled N-layer structural units, each layer of which consists of a two dimensional copper oxide plane. In the limit of infinite N, we recover essentially the usual Bloch wave description of a collection of copper oxide monolayers, aligned along the c axis.[10,13] Just as in the bilayer case, we find that there are

two competing states. Depending on the relative size of the intra and interplane coupling constants; one of the two is stable, while the other is metastable. These two limits correspond to inter and intralayer dominated states. In the band language the latter are in phase and the former out of phase. Because the system contains N such bands, the interlayer gap parameters should be viewed as sinusoidally modulated with varying band index, as will be illustrated in more detail below.

Just as in the bilayer case, the charge carriers within individual planes and on adjacent planes within a unit cell are assumed to interact via a nonretarded pair potential. Hopping of quasiparticles between adjacent planes within a unit cell is determined by the hopping matrix element $t_\perp$. No hopping is allowed between unit cells, as a consequence of our assumption that the c-axis coupling is incoherent. As before, only singlet intraband pair states are considered. Many of the detailed derivations in this section may be found in Appendix A 1.

The noninteracting Hamiltonian has the form

$$\hat{H}_N = \sum_\sigma \left[\sum_{i=1}^{N} \xi(\mathbf{q}) c_{i\sigma}^\dagger c_{i\sigma} - \sum_{i=1}^{N-1} (t_\perp c_{i\sigma}^\dagger c_{i+1,\sigma} + \text{c.c.}) \right],$$
(24)

where i is a layer and σ a spin index. The superconducting order parameter is defined by

$$\Delta_{ij}(\mathbf{q}) = \sum_{\mathbf{q}'} V_{ij}(\mathbf{q},\mathbf{q}') F_{ij}(\mathbf{q}'),$$
(25)

where V_{ij} is the interaction between electrons on layer i and layer j and the anomalous thermal Green's function $F_{ij}(\mathbf{q}) = \langle c_{i\uparrow}(\mathbf{q}) c_{j\downarrow}(-\mathbf{q}) \rangle$ is antisymmetrized with respect to spin indices. In this quantity $\langle \cdots \rangle$ indicates a Gibbs average.

The anomalous component of the superconducting Green's function is obtained by performing the usual matrix inversion

$$\mathscr{G}^{-1} = \begin{pmatrix} \iota\omega_l - H_N & -\Delta \\ -\Delta^* & \iota\omega_l + H_N \end{pmatrix}.$$
(26)

The entries in this matrix problem are $2N \times 2N$ matrices with two spin degrees of freedom and N layer indices, with $\omega = (2l+1)\pi\beta^{-1} \mathbb{1}_{2N}$.

We diagonalize Eq. (26) in the spin degrees of freedom by multiplying the entire equation from the right by σ_2. The equations are then transformed to the band picture by diagonalizing the normal state Hamiltonian H_N. The resulting energy dispersion in band r of the Hamiltonian is given by

$$\epsilon_r(\mathbf{q}) = \xi(\mathbf{q}) + 2t_\perp \cos\left(\frac{r\pi}{N+1}\right), \quad r = 1, \ldots, N. \quad (27)$$

We will consider only pairing of electrons within individual bands so that the order parameter is diagonal in the band representation with components Δ_r. With a fully diagonalized Green's function the gap equation for the N-layer system can now be readily obtained. Upon performing the sum over Matsubara frequencies, we find

$$\Delta_r(\mathbf{q}) = -\sum_{\mathbf{q}'} \sum_{r'=1}^{N} V^{r,r'}(\mathbf{q},\mathbf{q}') \frac{\Delta_{r'}(\mathbf{q}')}{2E_{r'}(\mathbf{q}')}$$
$$\times \tanh\left[\frac{1}{2}\beta E_{r'}(\mathbf{q}')\right].$$
(28)

The energy dispersion of the elementary excitations is given for each band r by the usual relation $E_r = \sqrt{\epsilon_r^2 + |\Delta_r|^2}$. Equation (28) is the central equation of this section. In Appendix A 3 we generalize this result further by extending it to an infinite stack of layers, corresponding to a fully three dimensional lattice.[69]

B. Solutions of the gap equation for small $t_\perp$

In this subsection we establish the nature of the two competing states which are the stable and metastable solutions to the gap equations derived from Eq. (28). These are most readily introduced by considering first the limit of small $t_\perp$. For arbitrarily small $t_\perp$, the two solutions become independent and appear with different onset or transition temperatures. These two states are respectively associated with pure intra and pure interlayer pairing. Moreover, in this limit analytical results can be obtained, while the more general case of nonzero $t_\perp$ is treated numerically.

After some algebra, which is outlined in Appendix A 2, it follows that the solution to the gap equation is given by

$$\Delta_r(\mathbf{q}) = \Delta_{\|,0} \psi_\|(\mathbf{q}) - 2\cos\left(\frac{r\pi}{N+1}\right) \Delta_{\perp,0} \psi_\perp(\mathbf{q}), \quad (29)$$

where the two Fermi surface functions $\psi_\|(\mathbf{q})$ and $\psi_\perp(\mathbf{q})$ satisfy

$$\Omega_\| \psi_\|(\mathbf{q}) = -\int \frac{dS}{(2\pi)^2 v_F} V_\|(\mathbf{q},\mathbf{q}') \psi_\|(\mathbf{q}'), \quad (30a)$$

$$\Omega_\perp \psi_\perp(\mathbf{q}) = -\int \frac{dS}{(2\pi)^2 v_F} V_\perp(\mathbf{q},\mathbf{q}') \psi_\perp(\mathbf{q}'). \quad (30b)$$

Here the integrations are over the degenerate bands of the Fermi surface and the related c numbers, $\Omega_\|$ and $\Omega_\perp$, are related to the respective transition temperatures $T_{\|/\perp,0}$ determined by the equation

$$\ln\left(\frac{1.14\omega_c}{k_B T_{\|/\perp,0}}\right) = \frac{1}{\Omega_{\|/\perp}}. \quad (31)$$

Finally, the two competing states are associated with taking either one of the two parameters in $\Delta_{\|,0}$ or $\Delta_{\perp,0}$ in Eq. (29) to be zero.

The above results can be generalized to the case of finite $t_\perp$, using numerical techniques. When $t_\perp$ is finite, the two parameters $\Delta_{\|,0}$ and $\Delta_{\perp,0}$ can be simultaneously nonzero in which case both $\psi_\|$ and $\psi_\perp$ will belong to the same irreducible representation of the lattice point group.

To illustrate these results, we plot the amplitudes on the various bands of the competing inter and intralayer pair states for $N=4$ and $N=7$ in Fig. 8. As in the bilayer case, if the dominant interaction is attractive then the order parameter will be nodeless, while a repulsive interaction will yield a nodal solution with exact form determined by the details of
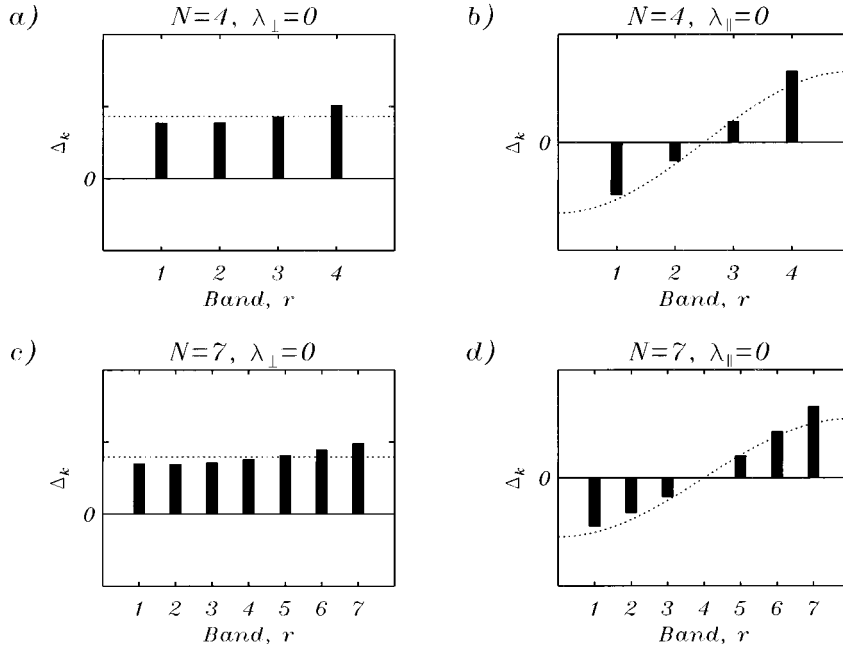
FIG. 8. Amplitude of pure intralayer and interlayer pairing solutions in the band representation for $N=4$ [(a) and (b), respectively] and $N=7$ [(c) and (d), respectively] cases. The ideal solutions ($t_\perp=0$) are denoted by the dotted lines and the actual solutions are calculated for moderately large $t_\perp$.

the interaction and the band structure (as discussed in Sec. II B 1). In panels (a) and (b) of Fig. 8 the magnitude of the order parameter is plotted as a function of band index r for the intraband (a) and interband (b) states for a four layer system. The dotted line indicates the analytical solution for $t_\perp=0$ and the histogram bars illustrate the numerical results for moderate $t_\perp$ (comparable in magnitude to the separation of the Fermi level from the van Hove points). In this way some deviation from the analytically obtained curve is seen as the solid bars differ slightly from the dotted line. It is clear that the two competing solutions represent a natural generalization of the bilayer results to an N-layer system. Similar results are plotted for the seven layer system in panels (c) and (d). It follows from the figures and the above discussion that in these higher N systems, even more complex behavior can be obtained, with a range of signs and magnitudes of the order parameters associated with the different bands.

To make this complexity even more explicit, we have considered the case of $N=3$ for the case of a dominant attractive interlayer interaction and a weak in-plane repulsion both peaked at (π,π). In this case the hopping is slightly larger than in the previous figure. Figure 9 shows our solution to the gap equation and the normal state band structure (inset) for this three band model of orthorhombic YBCO with the two lower energy bands closed about X and the highest energy band open. This last band can be viewed as simulating the chain band in YBCO,[23] since conduction in this band is only possible along one principle axis. Solution of the three layer gap equation clearly shows the mixing between the two components of the solution. The middle (planelike) band has a pure d-wave solution, since interlayer pairing contributes very little to the gap on this band, while the other two bands have s-wave symmetry. The physics of this three band model is equally complex. Because of the dominance of an s-wave order parameter component, one expects that the magnitude of T_c is only mildly affected by impurity scatterers. On the other hand, a nodal solution on one of the bands will yield power law dependences in ther-

modynamic functions at low temperatures. While the above model should not be viewed as a detailed representation of YBCO, it serves to illustrate the rich array of phenomena which are associated with multiband systems.

C. Basis functions and van Hove effects

Band structure effects have played an important role in our analysis, particularly when the Fermi energy lies in the vicinity of the van Hove singularities. We have seen that these singularities distort the shape of the order parameter. They also play a key role in determining the relative stability of various solutions to the gap equations. In this subsection we show that, of all the different gap symmetries, two are able to take maximal advantage of the van Hove points: these are the nodeless s if the interaction is attractive and the "$d_{x^2-y^2}$" states[70] in the case of a repulsive interaction. It should be noted that there is a considerable literature on the
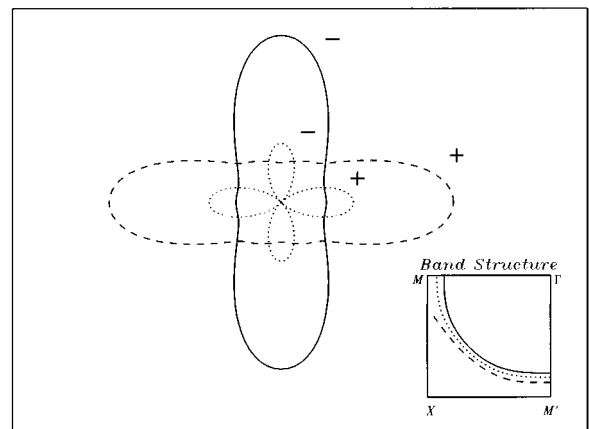

FIG. 9. Solution for a three band problem illustrating coexistence of solutions of different symmetries. The inset plots the associated band structure.

effect of the van Hove singularities on raising T_c.[71] In this paper we focus on the interplay of the van Hove singularity and order parameter symmetry. Earlier work[47,72] has shown that in the more general strong coupling picture, states far from the Fermi energy may wash out, to some degree, the effectiveness of the van Hove singularity in raising T_c. While here we use a weak coupling approach to address the order parameter symmetry the same qualitative behavior can be expected to follow in more general strong coupling calculations.

To quantify the van Hove effects we study the linearized form of Eq. (28)

$$\Omega \Delta_r(\mathbf{q}) = - \sum_{r'=1}^{N} \int_{\epsilon_{r'}=E_F} \frac{dS_{r'}}{(2\pi)^2 v_F^{r'}(\mathbf{q}')} V^{r,r'}(\mathbf{q},\mathbf{q}') \Delta_{r'}(\mathbf{q}'),$$

(32)

where the integrations are performed over segments of the Fermi surface corresponding to the different bands and the eigenvalue Ω defines the BCS transition temperature T_c:

$$\Omega^{-1} = \ln\left(\frac{1.14\omega_c}{k_B T_c}\right).$$

(33)

The Fermi velocity on band r is v_F^r, and E_F is the Fermi energy.

We define a complete set of orthonormal basis functions over the Fermi surface,[73] which are nonzero over only a single band r and assume further that these $\psi_i^{r(\Gamma)}(\mathbf{q})$ belong to an irreducible representation Γ of the lattice point group. These basis functions satisfy

$$\sum_{p=1}^{N} \int_{\epsilon_p=E_F} \frac{dS_p}{(2\pi)^2 v_F^p(\mathbf{q})} \psi_i^{r(\Gamma)}(\mathbf{q}) \psi_j^{r'(\Gamma')}(\mathbf{q}) = \delta_{i,j}\delta_{r,r'}\delta_{\Gamma,\Gamma'}.$$

(34)

The pair wave function and interaction potential[74] are expanded in terms of these Fermi surface harmonics as

$$\Delta_r = \sum_{\Gamma,i} \Delta_i^{r(\Gamma)} \psi_i^{r(\Gamma)},$$

(35)

and

$$V^{r,r'}(\mathbf{q},\mathbf{q}') = \sum_{\Gamma,i,j} V_{i,j}^{r,r'(\Gamma)} \psi_i^{r(\Gamma)}(\mathbf{q}) \psi_j^{r'(\Gamma)}(\mathbf{q}').$$

(36)

The gap equation is thus reduced to the simple set of eigenvalue problems

$$\Omega \Delta_i^{r(\Gamma)} = - \sum_{j,r'} V_{i,j}^{r,r'(\Gamma)} \Delta_j^{r'(\Gamma)}.$$

(37)

By working in the space of functions defined by Eq. (34) it is clear that the basis functions $\psi_i^{r(\Gamma)}$ are weighted by the inverse of $\sqrt{v_F^r}$ and so regions along the directions of the van Hove points give a correspondingly greater contribution in the gap equation. If the interaction $V^{r,r'}(\mathbf{q},\mathbf{q}')$ coupling two points on the Fermi surface is repulsive (attractive) then states with opposite (same) phase at these two points will be favored. Thus we conclude that the $d_{x^2-y^2}$ basis function will benefit most from the van Hove points for repulsive

$\alpha)$

PDOS

"s" (A_{1g})
"s_{xy}" (A_{1g})
"$d_{x^2-y^2}$" (B_{1g})
"d_{xy}" (B_{2g})
"g" (A_{2g})

$P(\Delta)$

$-0.38 \quad -0.24 \quad -0.10 \quad 0.04 \quad 0.18 \quad 0.32$
E_F

$b)$

PDOS Relative to $\Delta=1$

$P(\Delta)/P(1)$

2.0

1.0

0.0

$-0.38 \quad -0.24 \quad -0.10 \quad 0.04 \quad 0.18 \quad 0.32$
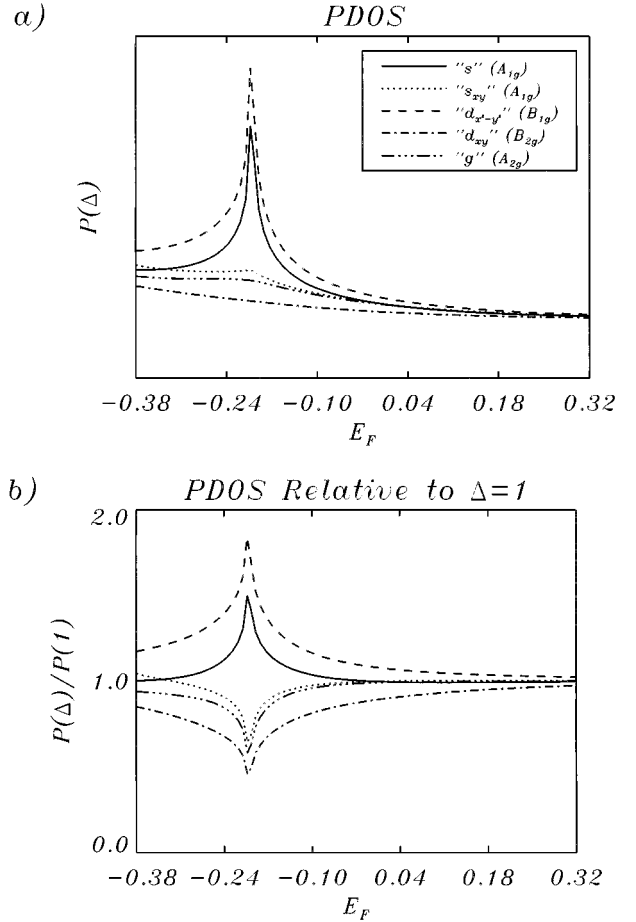E_F

FIG. 10. Pairing density of states (PDOS) of the solution with highest T_c in each irreducible representation for LSCO. Panel (a) shows the absolute PDOS in arbitrary units and panel (b) illustrates the PDOS normalized by the single particle density of states. The isotropic s state (solid line) was calculated for an attractive pair interaction peaked at (π,π) while the other solutions were calculated for repulsive interactions, with $\mathbf{Q}$ chosen so as to maximize T_c.

interactions while the nodeless s function will be most enhanced by an attractive interaction.

The effect of the van Hove singularities in the single particle density of states on the superconducting order parameter can be quantified through the pairing density of states (PDOS) (Ref. 75)

$$P_\Delta(E_F) = \frac{\int \frac{dS}{(2\pi)^2 v_F} |\Delta(\mathbf{q})|^2}{\int dS |\Delta(\mathbf{q})|^2}.$$

(38)

The integrals are taken over all bands of the Fermi surface. To illustrate this function and its relation to the van Hove singularities, in Fig. 10(a) we plot P_Δ as a function of the Fermi energy for various solutions to the gap equation. Here we focus on the one layer case for clarity. It can be seen that a peak appears at the van Hove point for all irreducible representations. It is, however, more appropriate to normalize by the single particle density of states $P_{\Delta=1}$. This gives a more

accurate indication of the degree to which the pair wave function is stabilized by the density of states. The result for the four different irreducible representations of the D_{4h} lattice of LSCO is plotted against Fermi energy in Fig. 10(b). Here we select that **Q** which results in a maximal T_c for each representation. In this way, we see that the B_{1g} solution, i.e., the "$d_{x^2-y^2}$" state, and the nodeless A_{1g} "s"-wave solution indeed benefit much more from the van Hove singularity than do all other states.

In summary, there are two states which take maximal advantage of the van Hove points. These are the nodeless s-wave state which occurs only for attractive interactions and the $d_{x^2-y^2}$ state, appropriate to the case of repulsive interactions. It should be stressed that in general the order parameter will not have these simple functional forms corresponding to a single basis function. This is all the more striking as the Fermi energy approaches the van Hove singularity where admixtures of higher order basis functions are most evident. While in the presence of multiple bands, the results plotted in Fig. 10 become more complicated, the essential features still remain.

IV. CONCLUSION

The most important issues in the field of high-T_c superconductivity involve determinations of the order parameter symmetry and the superconducting pairing mechanism. While there are, clearly, no definitive answers to be had at this time, this paper has been directed towards addressing these two issues. We have emphasized the role of multilayer effects in the cuprates, in large part because the most well characterized material, YBCO, has two copper oxide planes. This complexity leads to complications in inferring the order parameter symmetry from various experimental tests. It also suggests that there are different (inter- and intraplane) channels which should be considered in any microscopic theory of the pairing.

In reference to the order parameter symmetry, we have found that a multilayer system should be characterized by distinct gaps appropriate to each of the multiple bands. A bilayer material such as YBCO has two gaps, a trilayer, three, etc. In the presence of even a very small amount of orthorhombicity, one of the gaps can be predominantly of d, while another of s symmetry. (Throughout this paper we refer to d and s states as those which are odd or even, respectively, under a $\pi/2$ rotation of the wave vector.) One may be nodeless while the other has nodes. The multiple gaps can be in or out of phase. In this way the observation of power law behavior in thermodynamics may reflect on only one of the order parameters in question. The observation of π phase shifts in Josephson corner junction experiments on YBCO must be viewed more widely in this multiband context. Indeed, we have found that this behavior can be associated with two out of phase s states in the presence of (weak) orthorhombicity. This orthorhombicity leads to a strong asymmetry of the s and $-s$ states, so that one gap function is elongated along the a and the other along the b axes of the crystal. The net Josephson current behaves rather similarly to a $d_{x^2-y^2}$ state, although the thermodynamical behavior need not exhibit the power laws of this state. Finally, the behavior of multilayer systems in the presence of

impurities is similarly complex. Intra and interlayer impurities suppress T_c in a different fashion. The $(s, -s)$ state is of interest because it obeys an Anderson theorem with respect to interlayer substitutions. This may help explain why substitutions at the rare earth site in YBCO make little or no difference to the magnitude of T_c.

In the process of investigating very generic model interactions for the superconductivity, we have inferred information about microscopic constraints on the pairing mechanism. $d_{x^2-y^2}$-like states are found to be general solutions to the gap equation for repulsive interactions, in large part because they possess the fewest number of nodes and thereby the highest transition temperatures. In this way, they should not be specifically associated with a spin fluctuation driven pairing mechanism. Moreover, van Hove effects act to stabilize some order parameters over others. Of these the $d_{x^2-y^2}$-like symmetry is, again, the most notable. Orthorhombicity further enhances this stabilization. Thus for a variety of reasons, this state emerges as a natural solution to the gap equation(s) in the presence of repulsive interactions.

While we have emphasized the bilayer ($N=2$) case, we also presented general multilayer calculations which view the c axis as consisting of decoupled structural units, each of which contains N copper oxide layers. By contrast, within the unit cell the intra- and interplane hopping is appreciable and plays an important role in giving rise to N distinct bands. These $N>2$ calculations may be particularly relevant in the context of the Hg and Bi based cuprates. In treating the superconductivity, we have included intra- and interplane pairing interactions in parallel with the above intra- and interplane hopping. We demonstrated that, regardless of the number of layers N in the unit cell, there are always two competing states: one of which is intraplane dominated, so that the resulting N band gaps are in phase, and one of which is interplane dominated, so that the N gaps are sinusoidally modulated. Small changes in the parametrizations can lead to a transition from one of these states to another. Thus it may be inferred that the order parameter symmetry is potentially variable from one cuprate to another and from one stoichiometry to another.

While the inclusion of these multilayer effects has been seen to introduce considerable complexity into the classification of the order parameter symmetry, this complexity is inescapable. As long as the layers communicate via one or two body processes (i.e., via hopping or pairing interactions), superconductivity in the high-T_c cuprates must include these multilayer effects.

ACKNOWLEDGMENTS

APPENDIX A: CALCULATION OF GAP EQUATION FOR N LAYERS

1. Derivation

To begin we need to calculate the superconducting Green's function defined by the $4N \times 4N$ matrix

$$\mathscr{G}^{-1}=\begin{pmatrix} \iota\omega_l-H_N & -\Delta \\ -\Delta^* & \iota\omega_l+H_N \end{pmatrix}. \qquad (A1)$$

The components H_N and Δ are defined in Sec. III A. First we diagonalize the normal state Hamiltonian. For this purpose we define the set of characteristic polynomials

$$D_N(\xi-\epsilon)=\det(H_N-\epsilon\mathbb{1}_N) \qquad (A2)$$

and observe that they satisfy the recursion relation

$$D_i(x)=xD_{i-1}(x)-t_\perp^2 D_{i-2}(x),$$
$$D_0(x)=0,$$
$$D_1(x)=x. \qquad (A3)$$

By using the known properties of the Chebyshev polynomials it is straightforward to show that these characteristic polynomials have the form

$$D_N(x)=(-t_\perp)^N\frac{\sin[(N+1)q]}{\sin(q)},$$
$$x=-2t_\perp\cos(q). \qquad (A4)$$

From the zeros of these polynomials we can determine the normal state energies

$$\epsilon_r(\mathbf{q})=\xi(\mathbf{q})+2t_\perp\cos\left(\frac{r\pi}{N+1}\right),r=1,\ldots,N. \qquad (A5)$$

An orthonormal set of eigenstates of H_N can be found similarly. The ith component of the state associated with band r is given by

$$\phi_i^r=\sqrt{\frac{2}{N+1}}(-1)^{i+r}\sin\left(\frac{ir\pi}{N+1}\right) \qquad (A6)$$

and consequently the components of the unitary matrix which diagonalizes (39) are given by

$$U_{ij}=\sqrt{\frac{2}{N+1}}(-1)^{i+j}\sin\left(\frac{ij\pi}{N+1}\right). \qquad (A7)$$

The particle creation operators in the band and layer language are thus related by the equation

$$a_i^\dagger=\sum_{j=1}^N U_{ij}c_j^\dagger. \qquad (A8)$$

Since we predominantly focus on intraband pairing the order parameter associated with each band r is thus defined through the anomalous thermal Green's function components

$$F_{r,r'}(\mathbf{q})=\frac{1}{\sqrt{2}}\langle a_{r\uparrow}(\mathbf{q})a_{r'\downarrow}(-\mathbf{q})-a_{r\downarrow}(\mathbf{q})a_{r'\uparrow}(-\mathbf{q})\rangle$$
$$=\frac{2}{N+1}\sum_{i=1}^N\sum_{j=1}^N(-1)^{i+j}\sin\left(\frac{ir\pi}{N+1}\right)\sin\left(\frac{jr'\pi}{N+1}\right)$$
$$\times F_{i,j}(\mathbf{q})\delta_{r,r'}. \qquad (A9)$$

We thus define the N diagonal components of the order parameter in the band language Δ_r by the equation

$$\Delta_r=\frac{2}{N+1}\sum_{i=1}^N\sum_{j=1}^N(-1)^{i+j}\sin\left(\frac{ir\pi}{N+1}\right)\sin\left(\frac{jr\pi}{N+1}\right)\Delta_{i,j}. \qquad (A10)$$

With the pairing restricted to intralayer pairing and pairing between nearest neighbor planes we can use the definition of $\Delta_{i,j}$ to write the order parameter on a given band r in terms of the anomalous part of the Green's function

$$\Delta_r(\mathbf{q})=\frac{1}{N+1}\sum_{\mathbf{q}'}\left\{\sum_{i=1}^N V_\parallel(\mathbf{q},\mathbf{q}')\sin\left(\frac{ir\pi}{N+1}\right)\sin\left(\frac{ir'\pi}{N+1}\right)F_{ii}(\mathbf{q}')\right.$$
$$\left.-2\sum_{i=1}^{N-1}V_\perp(\mathbf{q},\mathbf{q}')\sin\left(\frac{ir\pi}{N+1}\right)\sin\left(\frac{(i+1)r\pi}{N+1}\right)[F_{i,i+1}(\mathbf{q}')+F_{i+1,i}(\mathbf{q}')]\right\}. \qquad (A11)$$

With a fully diagonalized Green's function the gap equation for the N-layer system can now be readily obtained. Upon performing the sum over Matsubara frequencies in the usual way we get

$$\Delta_r(\mathbf{q})=-\sum_{\mathbf{q}'}\sum_{r'=1}^N V^{r,r'}(\mathbf{q},\mathbf{q}')\frac{\Delta_{r'}(\mathbf{q}')}{2E_{r'}(\mathbf{q}')}\tanh\left[\frac{1}{2}\beta E_{r'}(\mathbf{q}')\right], \qquad (A12)$$

where the interaction in the band representation is defined as

$$V^{r,r'}(\mathbf{q},\mathbf{q}')=\frac{1}{N+1}\left\{[1+\tfrac{1}{2}\theta_{r,r'}^{+(N)}]V_\parallel(\mathbf{q},\mathbf{q}')+\left[2\cos\left(\frac{r\pi}{N+1}\right)\cos\left(\frac{r'\pi}{N+1}\right)+\theta_{r,r'}^{-(N)}\right]V_\perp(\mathbf{q},\mathbf{q}')\right\},$$

$$\theta_{r,r'}^{\pm(N)}=\delta_{r,r'}\pm\delta_{r+r',N+1}. \qquad (A13)$$

The quasiparticle dispersions in the superconducting state are defined by the usual relation $E_r = \sqrt{\epsilon_r^2 + |\Delta_r|^2}$.

2. The small $t_\perp$ limit

For infinitesimal $t_\perp$ it is interesting to transform Eq. (A12) to the layer representation using Eq. (A10). Then to zeroth order in $t_\perp$ the N intralayer problems uncouple from the $N-1$ interlayer problems yielding the following two sets of gap equations:

$$\Delta_{i,i}(\mathbf{q}) = \frac{-1}{N+1}\sum_{\mathbf{q}'} V_\parallel(\mathbf{q},\mathbf{q}')\frac{\tanh[\frac{1}{2}\beta E(\mathbf{q}')]}{2E(\mathbf{q}')}$$

$$\times \sum_{j=1}^{N} (1 + \tfrac{1}{2}\theta_{i,j}^{+(N)})\Delta_{j,j}(\mathbf{q}'), \quad \text{(A14a)}$$

$$\Delta_{i,i+1}(\mathbf{q}) = \frac{-1}{N+1}\sum_{\mathbf{q}'} V_\perp(\mathbf{q},\mathbf{q}')\frac{\tanh[\frac{1}{2}\beta E(\mathbf{q}')]}{2E(\mathbf{q}')}$$

$$\times \sum_{j=1}^{N-1} (1 + \theta_{i,j}^{+(N-1)})\Delta_{j,j+1}(\mathbf{q}'). \quad \text{(A14b)}$$

Linearizing with respect to Δ and solving for the eigenvalues and eigenfunctions of these two equations gives the T_c's of the various pairing states available to the system and only one of these solutions will correspond to the maximal value of T_c.

Let us first define two functions on the Fermi surface, $\psi_\parallel(\mathbf{q})$ and $\psi_\perp(\mathbf{q})$, and two numbers, $\Omega_\parallel$ and $\Omega_\perp$, which satisfy the two equations

$$\Omega_\parallel \psi_\parallel(\mathbf{q}) = -\int \frac{dS}{(2\pi)^2 v_F} V_\parallel(\mathbf{q},\mathbf{q}')\psi_\parallel(\mathbf{q}'), \quad \text{(A15a)}$$

$$\Omega_\perp \psi_\perp(\mathbf{q}) = -\int \frac{dS}{(2\pi)^2 v_F} V_\perp(\mathbf{q},\mathbf{q}')\psi_\perp(\mathbf{q}'). \quad \text{(A15b)}$$

The integrations are over the degenerate bands of the Fermi surface. The pair amplitudes can be written in the form

$$\Delta_{i,i}(\mathbf{q}) = \Delta_\parallel^i \psi_\parallel(\mathbf{q}),$$
$$\Delta_{i,i+1}(\mathbf{q}) = \Delta_\perp^i \psi_\perp(\mathbf{q}). \quad \text{(A16)}$$

The gap equations (A14) are transformed in the usual manner by separating the sum over quasimomenta to separate integrals over energy and the Fermi surface. The energy integral can then be performed to obtain a BCS-like transition temperature and using Eqs. (A15) we derive the linear matrix equations

$$\Delta_\parallel^i = \ln\left(\frac{\gamma\omega_c}{k_B T_c}\right)\frac{\Omega_\parallel}{N+1}\sum_{j=1}^{N}(1+\tfrac{1}{2}\theta_{i,j}^{+(N)})\Delta_\parallel^j, \quad \text{(A17a)}$$

$$\Delta_\perp^i = \ln\left(\frac{\gamma\omega_c}{k_B T_c}\right)\frac{\Omega_\perp}{N+1}\sum_{j=1}^{N-1}(1+\theta_{i,j}^{+(N-1)})\Delta_\perp^j, \quad \text{(A17b)}$$

where $\gamma \approx 1.14$ and ω_c is the usual cutoff energy. We can now characterize all the available pairing states with functional form given by $\psi_\parallel$ and $\psi_\perp$ along with their BCS transition temperatures.

Equations (A17) each have one isotropic eigenvector given by $\Delta_{\parallel/\perp}^i = \Delta_{\parallel/\perp,0}$ with $T_{c,0}$ determined by the equation

$$\ln\left(\frac{\gamma\omega_c}{k_B T_{c,0}}\right) = \frac{1}{\Omega_{\parallel/\perp}}, \quad \text{(A18)}$$

which give the most stable candidate pairing states for the two mechanisms. The remaining eigenvectors correspond either to metastable states which are symmetric in the layer index such that $\Sigma_i \Delta_{\parallel/\perp}^i = 0$ with T_c given by

$$\ln\left(\frac{T_c}{T_{c,0}}\right) = \begin{cases} -\dfrac{N}{\Omega_\parallel} \\ -\dfrac{N-1}{2\Omega_\perp} \end{cases}, \quad \text{(A19)}$$

or nonpairing states ($T_c = 0$) which are odd in the layer index.

Transforming to the band picture using Eq. (A10) we find that the intralayer pairing states are even under the transformation $r \to N+1-r$ whereas the interlayer pairing states are odd under this transformation. The two most stable candidate states thus give a superconducting order parameter of the form

$$\Delta_r(\mathbf{q}) = \Delta_{\parallel,0}\psi_\parallel(\mathbf{q}) - 2\cos\left(\frac{r\pi}{N+1}\right)\Delta_{\perp,0}\psi_\perp(\mathbf{q}). \quad \text{(A20)}$$

The two parameters $\Delta_{\parallel,0}$ and $\Delta_{\perp,0}$ are both nonzero only when $t_\perp$ is finite and when $\psi_\parallel$ and $\psi_\perp$ belong to the same irreducible representation. Since the two different pairing mechanisms give solutions of different r dependence, the dominant type of pairing can be easily determined even when $t_\perp$ is finite. Mixing of solutions at finite $t_\perp$ and the effect on the transition temperature is discussed in Appendix B in the bilayer context.

3. Formulation in terms of Bloch waves

For completeness we conclude by relating the above formulation to the usual treatment of layered materials. It would be natural to define a z component of the quasimomentum vector to be

$$q_z = \frac{r\pi}{N+1}. \quad \text{(A21)}$$

Note, however, that there are N linearly independent, nondegenerate eigenstates for $0 < q_z < \pi$ and so taking $q_z \to -q_z$ gives no new states. Thus interpreting q_z as a momentum is rather unnatural.

The usual procedure in the case of large N,[10,13] however, is to assume periodic boundary conditions. This means that we have hopping between layers 1 and N and that the system is translationally invariant along the c axis. The eigenstates of this new Hamiltonian are

$$\phi_j^r = \frac{1}{\sqrt{N}} \exp\left(\iota \frac{2r\pi}{N} j \right), \quad \text{(A22)}$$

with energies

$$\epsilon_r = \xi + 2t_\perp \cos\left(\frac{2r\pi}{N} \right). \quad \text{(A23)}$$

Taking the limit of N going to infinity one obtains the gap equation for a fully three dimensional system. Again assuming only intraband pairing the gap equation becomes

$$\Delta(\mathbf{q}) = -\sum_{\mathbf{q}'} V(\mathbf{q},\mathbf{q}') \frac{\Delta(\mathbf{q}')}{2E(\mathbf{q}')} \tanh\left[\frac{1}{2}\beta E(\mathbf{q}') \right], \quad \text{(A24)}$$

with the interaction

$$V(\mathbf{q},\mathbf{q}') = \frac{1}{N}[V_\parallel(\mathbf{q},\mathbf{q}') + 2\cos(q_z - q_z')V_\perp(\mathbf{q},\mathbf{q}')], \quad \text{(A25)}$$

and the usual quasiparticle energies $E(\mathbf{q}) = \sqrt{\epsilon(\mathbf{q})^2 + |\Delta(\mathbf{q})|^2}$. In the large N limit this system behaves identically to the one considered throughout this paper when only singlet pairing is considered. On the other hand, it is obvious that this formulation gives very different results in the small N limit. One might expect that in any real system the hopping between unit cells is different from that within a unit cell and so a more general formulation than either of these would be required. Such a formulation would, however, yield a continuous set of Fermi levels within some small band and this result would be in contradiction to experimental observations.

APPENDIX B: INTERBAND PAIRING

To conclude this discussion we present a more careful treatment of the case for which $N=2$ admitting the possibility of pairing of electrons on different subbands of the Fermi surface. We will restrict our attention to states which are even under inversion, neglecting the possibility of a p-wave order parameter. This necessitates the consideration of a triplet interlayer pairing state. The normal state Hamiltonian has the form

$$H_2 = \begin{pmatrix} \xi & -t_\perp \\ -t_\perp^* & \xi \end{pmatrix}, \quad \text{(B1)}$$

where $t_\perp = |t_\perp| e^{-\iota\varphi}$. The order parameter has the form

$$\Delta = \begin{pmatrix} \Delta_\parallel^e + \Delta_\parallel^o & \Delta_\perp^s - \iota\sum_{i=1}^{3} \Delta_\perp^{t,i}\sigma_i \\ \Delta_\perp^s + \iota\sum_{i=1}^{3} \Delta_\perp^{t,i}\sigma_i & \Delta_\parallel^e - \Delta_\parallel^o \end{pmatrix}. \quad \text{(B2)}$$

The σ_i are the three Pauli spin matrices. Upon diagonalizing (64) we obtain

$$H_2 = \begin{pmatrix} \xi - |t_\perp| & 0 \\ 0 & \xi + |t_\perp| \end{pmatrix}, \quad \text{(B3)}$$

$$\Delta = \begin{pmatrix} \Delta_+ & \Delta_1 - \iota\Delta_2 \\ \Delta_1 + \iota\Delta_2 & \Delta_- \end{pmatrix}. \quad \text{(B4)}$$

We assume that the triplet component is describable by a single complex parameter $\Delta_\perp^t$ and a real unit vector in spin space $\hat{n}$ so that $\Delta_\perp^{t,i} = \Delta_\perp^t \hat{n}_i$. The Green's function can thus be diagonalized in its spin degrees of freedom. There are, therefore, four independent parameters which describe the superconducting state. The components of the order parameter in the band representation are

$$\Delta_+ = \Delta_\parallel^e + \Delta_\perp^s,$$
$$\Delta_- = \Delta_\parallel^e - \Delta_\perp^s,$$
$$\Delta_1 = \Delta_\parallel^o,$$
$$\Delta_2 = -\Delta_\perp^t \sigma_3. \quad \text{(B5)}$$

Designating the bands by $\epsilon_\pm = \xi \mp |t_\perp|$ we solve for the anomalous parts of the Green's function as before. These may be linearized in Δ at T_c and upon performing the sum over Matsubara frequencies we arrive at the following four gap equations:

$$\Delta_+ + \Delta_- = -\sum_{\mathbf{q}} V_\parallel \left[\Delta_+ \frac{\tanh(\frac{1}{2}\beta\epsilon_+)}{2\epsilon_+} + \Delta_- \frac{\tanh(\frac{1}{2}\beta\epsilon_-)}{2\epsilon_-} \right], \quad \text{(B6a)}$$

$$\Delta_+ - \Delta_- = -\sum_{\mathbf{q}} V_\perp \left[\Delta_+ \frac{\tanh(\frac{1}{2}\beta\epsilon_+)}{2\epsilon_+} - \Delta_- \frac{\tanh(\frac{1}{2}\beta\epsilon_-)}{2\epsilon_-} \right], \quad \text{(B6b)}$$

$$\Delta_1 = -\sum_{\mathbf{q}} V_\parallel \Delta_1 \frac{\tanh(\frac{1}{2}\beta\epsilon_+) + \tanh(\frac{1}{2}\beta\epsilon_-)}{2\epsilon_+ + 2\epsilon_-}, \quad \text{(B6c)}$$

$$\Delta_2 = -\sum_{\mathbf{q}} V_\perp \Delta_2 \frac{\tanh(\frac{1}{2}\beta\epsilon_+) + \tanh(\frac{1}{2}\beta\epsilon_-)}{2\epsilon_+ + 2\epsilon_-}. \quad \text{(B6d)}$$

If $t_\perp = 0$ then there is a single transition temperature associated with the two intralayer pairing states and another transition temperature associated with the two interlayer states. Denote the larger one of these by $T_{c,0}$. It can be shown that for nonzero $t_\perp$ the transitions described by Eqs. (B6c) and (B6d) have a lower T_c than the intraband pairing state transition in Eqs. (B6a) and (B6b) where for small $t_\perp$ the new transition of the interband pairing state[76,62] with higher T_c is given in terms of $T_{c,0}$ by

$$\ln\left(\frac{T_c}{T_{c,0}} \right) = -0.2123 \left(\frac{t_\perp}{k_B T_c} \right)^2. \quad \text{(B7)}$$

The transition temperature for the intraband pairing states is given by

$$\ln\left(\frac{T_c}{T_{c,0}} \right) = \frac{1}{\left| \ln\frac{T_{c,\parallel}}{T_{c,\perp}} \right|} \left(\frac{t_\perp R}{2k_B T_c} \right)^2, \quad \text{(B8)}$$

where the overlap between the two pair wave functions is

$$R = \int \frac{dS}{(2\pi)^2 v_F} \psi_\parallel \psi_\perp. \quad \text{(B9)}$$

We thus see that in the presence of interlayer tunneling the favored pairing state is always an intraband pairing state.

[1] D. J. Scalapino, Phys. Rep. **250**, 329 (1995).

[2] R. C. Dynes, Solid State Commun. **92**, 53 (1994).

[3] K. Levin, Y. Zha, R. J. Radtke, Q. Si, M. R. Norman, and H.-B. Schüttler, J. Supercond. **7**, 563 (1994).

[4] Z.-X. Shen *et al.*, Phys. Rev. Lett. **70**, 1553 (1993).

[5] M. R. Norman, M. Randeria, H. Ding, J. C. Campuzano, and A. F. Bellman (unpublished). See also Ding *et al.*, Phys. Rev. Lett. **75**, 1425 (1995).

[6] J. C. Campuzano *et al.*, Phys. Rev. Lett. **64**, 2308 (1990); R. Liu *et al.*, Phys. Rev. B **46**, 11 056 (1992).

[7] H. Ding *et al.*, the conclusions reached here regarding the absence of bilayer splitting disagree with those of Ref. 4 (unpublished).

[8] D. Z. Liu, K. Levin, and J. Maly, Phys. Rev. B **51**, 8680 (1995).

[9] A. I. Liechtenstein, I. I. Mazin, and O. Andersen, Phys. Rev. Lett. **74**, 2303 (1995).

[10] R. A. Klemm and S. H. Liu, Phys. Rev. B **44**, 7526 (1991).

[11] N. Bulut, D. J. Scalapino, and R. T. Scalettar, Phys. Rev. B **45**, 5577 (1992).

[12] L. N. Bulaevskii and M. V. Zyskin, Phys. Rev. B **42**, 10 230 (1990).

[13] S. Kettemann and K. B. Efetov, Phys. Rev. B **46**, 8515 (1992).

[14] C. C. Tsuei, J. R. Kirtley, C. C. Chi, L. S. Yu-jahnes, A. Gupta, T. Shaw, J. Z. Sun, and M. B. Ketchen, Phys. Rev. Lett. **73**, 593 (1994).

[15] D. A. Brawner and H. R. Ott (unpublished).

[16] D. A. Wollman, D. J. Van Harlingen, W. C. Lee, D. M. Ginsberg, and A. J. Leggett, Phys. Rev. Lett. **71**, 2134 (1993).

[17] A. Mathai, Y. Gin, R. C. Black, A. Amar, and F. C. Wellstood, Phys. Rev. Lett. **74**, 4523 (1995).

[18] J. Ma *et al.*, Phys. Rev. B **51**, 3832 (1995).

[19] C. C. Tsuei, D. M. Newns, J. R. Kirtley, and P. C. Pattnaik (unpublished). These authors have reached a similar conclusion.

[20] A. A. Golubov and I. I. Mazin, Physica C **243**, 153 (1995).

[21] Q. P. Li, B. E. C. Koltenbah, and R. Joynt, Phys. Rev. B **48**, 437 (1993).

[22] K. Kobuki and P. A. Lee (unpublished).

[23] I. I. Mazin, A. A. Golubov, and A. D. Zaikin, Phys. Rev. Lett. **75**, 2574 (1995).

[24] V. L. Pokrovsky (unpublished).

[25] R. Combescot and X. Leyronas, Phys. REv. Lett. **75**, 3732 (1995).

[26] S. L. Cooper and K. E. Gray, in *Physical Properties of High-Temperature Superconductors IV*, edited by D. M. Ginsberg (World Scientific, Singapore, 1994).

[27] P. W. Anderson, Phys. Rev. Lett. **67**, 660 (1991).

[28] A. G. Rojo and K. Levin, Phys. Rev. B **48**, 16 861 (1993).

[29] K. B. Efetov and A. I. Larkin, Sov. Phys. JETP **41**, 76 (1975).

[30] S. Chakravarty and P. W. Anderson, Phys. Rev. Lett. **72**, 3858 (1994).

[31] J. Rossat-Mignon *et al.*, Physica C **185**, 86 (1991).

[32] J. M. Tranquada, P. M. Gehring, and G. Shirane, Phys. Rev. B **46**, 5561 (1992).

[33] H. A. Mook, M. Yethiraj, G. Aeppli, T. E. Mason, and T. Armstrong, Phys. Rev. Lett. **70**, 3490 (1993).

[34] Y. Zha, Q. Si, and K. Levin, Physica C **212**, 418 (1993).

[35] Electronic coupling of copper-oxide planes was considered in Ref. 32.

[36] J. Schabel *et al.* (unpublished).

[37] D. Pines and P. Monthoux, *The Proceedings of the Stanford Conference on Spectroscopy in Novel Superconductors* (Pergamon Press, New York, 1995) [J. Phys. Chem. Solids (to be published)].

[38] A. J. Millis, S. Sachdev, and C. M. Varma, Phys. Rev. B **37**, 4975 (1988).

[39] R. J. Radtke, K. Levin, H.-B. Schüttler, and M. R. Norman, Phys. Rev. B **48**, 653 (1993).

[40] A. J. Leggett, Physica B **199−200**, 291 (1994).

[41] A. G. Sun, L. M. Paulius, D. A. Gajewski, M. B. Maple, and R. C. Dynes, Phys. Rev. B **50**, 3266 (1994).

[42] O. K. Andersen, A. I. Liechtenstein, O. Jepsen, and F. Paulsen (unpublished).

[43] A. A. Abrikosov, Physica C **244**, 243 (1995).

[44] C. M. Varma, *The Proceedings of the Stanford Conference on Spectroscopy in Novel Superconductors* (Ref. 37).

[45] In BSCCO, superlattice effects result in two nonequivalent Cu sites. Thus the unit cell is face-centered orthorhombic and double the size of the YBCO unit cell with the orthorhombic axes rotated by 45°. For simplicity, we simulate this lattice by a unit cell which has "rhombohedral" symmetry, with a unit cell equivalent to that in YBCO, but with rotated axes of symmetry.

[46] N. Fukushima, H. Niu, S. Nakamura, S. Takeno, M. Hayashi, and K. Ando, Physica C **159**, 777 (1989). These authors noted that upon addition of Pb, BSCCO acquired a mild rhombohedral distortion.

[47] R. J. Radtke and M. R. Norman, Phys. Rev. B **50**, 9554 (1994), we use the YBCO(1,ext) band structure in the case of YBCO.

[48] D. Sahu, A. Langner, and T. F. George, Phys. Rev. B **38**, 2466 (1988).

[49] M. U. Ubbens and P. A. Lee, Phys. Rev. B **50**, 438 (1994).

[50] B. Normand, H. Kohno, and H. Fukuyama (unpublished).

[51] Since the system is assumed orthorhombic all states are s-d mixed states; however, the order parameter on a given band will have same (opposite) sign under $\pi/2$ rotation if the s (d) component dominates.

[52] A. G. Sun, D. A. Gajewski, M. B. Maple, and R. C. Dynes, Phys. Rev. Lett. **72**, 2267 (1994).

[53] C. O'Donovan, D. Branch, J. P. Carbotte, and J. Preston, Phys. Rev. B **51**, 6588 (1995).

[54] V. Ambegaokar and A. Baratoff, Phys. Rev. Lett. **10**, 486 (1963).

[55] E. L. Wolf, *Principles of Electron Tunneling Spectroscopy* (Oxford University Press, New York, 1985).

[56] L. J. Buchholtz, M. Palumbo, D. Rainer, and J. A. Sauls (unpublished).

[57] C. C. Tsuei, J. R. Kirtley, M. Rupp, J. Z. Sun, A. Gupta, M. B. Ketchen, C. A. Wang, Z. F. Ren, and J. H. Wang (private communication).

[58] This effect is illustrated in Fig. 5 and proven in Sec. III C. Density of states contributions in general cancel out of $r_{\pm}$ in Eq. (10). An exception occurs when the tunneling barrier is modeled by a delta function potential as in Ref. 23 in which case $r_{\pm}$ is inversely proportional to the normal component of the Fermi velocity. In this case, tunneling is somewhat suppressed from the antibonding band and considerably enhanced from chain bands, as these authors point out.

[59] T. M. Rice (private communication).

[60] V. K. Vlasko-Vlasov *et al.*, Phys. Rev. Lett. **72**, 3246 (1994).

[61] It should be noted that there are two more general coupling terms which could, in principle, be added to the quartic contribution (Refs. 48,62). These terms do not appear in mean field theory when only pairing of electrons in a single band are considered. The analogous terms in the layer language however are present.

[62] M. Sigrist and T. M. Rice, Z. Phys. B. Condens. Matter **68**, 9 (1987).

[63] When $t_\perp$ is small γ' is $0.8525/(k_B T_c)^2$ where T_c is the larger of the two transition temperatures and $\beta' = 4\gamma'$.

[64] If $\delta = 0$ then the sign is undetermined.

[65] R. A. Klemm and K. Scharnberg, Phys. Rev. B **24**, 6361 (1981).

[66] Scattering by Zi and Ni impurities within the copper-oxide planes and the resulting T_c suppression is discussed in a monolayer context in Ref. 37.

[67] Calculating the suppression of T_c yields a result similar to that of Kettemann and Efetov (Ref. 13).

[68] Finding the suppression of T_c gives a straightforward extension of the usual result (Ref. 39). Furthermore one finds that if the impurity preferentially scatters electrons on one band, then the pairing amplitude is increased on the other band.

[69] R. J. Radtke, A. I. Liechtenstein, V. M. Yakovenko, and S. Das Sarma (unpublished).

[70] C. C. Tsuei, D. M. Newns, J. R. Kirtley, and P. C. Pittnaik (unpublished).

[71] D. M. Newns, C. C. Tsuei, P. C. Pittnaik, and C. I. Kane, Condens. Matter Phys. **15**, 273 (1992).

[72] R. J. Radtke, K. Levin, H.-B. Schüttler, and M. R. Norman, Phys. Rev. B **48**, 15 957 (1993).

[73] P. B. Allen, Phys. Rev. B **13**, 1416 (1976).

[74] K. Aoi and J. C. Swihart, Phys. Rev. B **7**, 1240 (1972).

[75] R. Fehrenbacher and M.R. Norman, Phys. Rev. Lett. **74**, 3884 (1995).

[76] Note that for interband pairing to occur we require $|t_\perp| < \omega_c$ since only pairing between time reversed states is being considered.